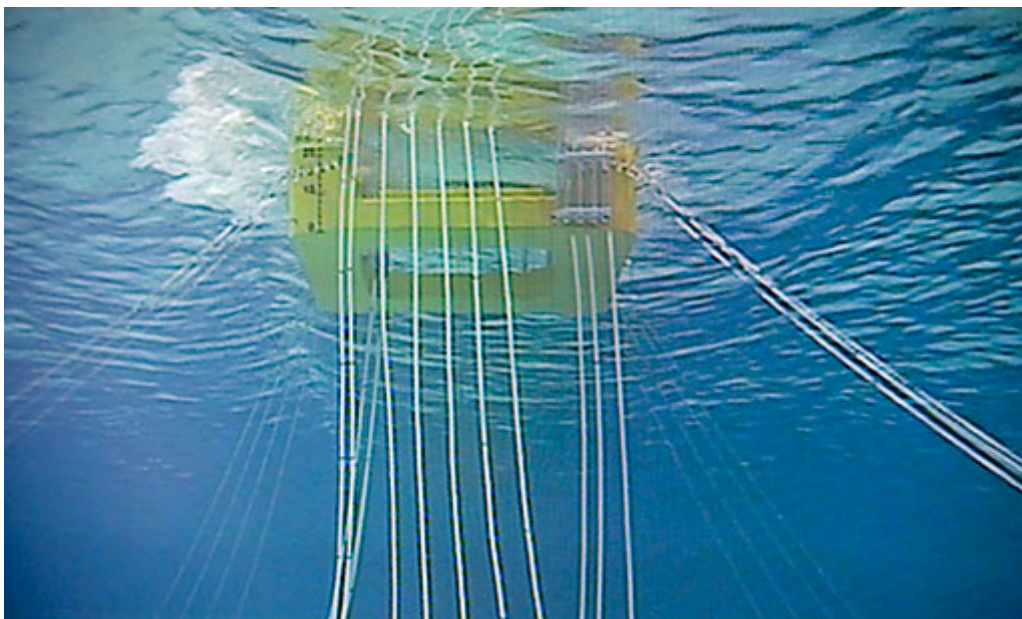


Master Thesis

**Second Order Drift Effects on a
Floating Construction**



School of Engineering and Science
M.Sc. in Civil and Structural Engineering
Aalborg University

Stefan Arenfeldt Vilsen

June 10, 2013

Master Thesis

Title:

Second Order Drift Effects on a Floating Construction

Written by:

Stefan Arenfeldt Vilsen

Graduate Student

School of Engineering and Science

M.Sc. in Structural and Civil Engineering

Supervisor:

Professor Peter Bak Frigaard

Project Period: Autumn 2012 - Spring 2013

Completed: 10th of June 2013

Copies printed: 3

Number of pages: 49

Number of Appendices: 13

Stefan Arenfeldt Vilsen

The content of the report is freely available, but publication (with source reference) is only allowed with agreement by the authors.

The frontpage picture is from [SINTEF].

Preface

This report is written as a Master Thesis by Stefan Arenfeldt Vilsen, at the department of Structural and Civil Engineering at Aalborg University. The project contains results from laboratory testing performed at University of Padova in Italy.

The project consists of two parts, a main report and an appendix report. The main report is intended to be read through, as a presentation of the methods and results from the project. The appendix report contains additional data and results from the laboratory preparations and testing. References in the main report are presented in a bibliography in the back of the report. In the main report, the references are listed by the *Harvard Method*.

I would like to thank for the help and support, received by Professor Luca Martinelli and Professor Piero Ruol during my stay at University of Padova.

Summary

In this project the aim is to document the presence of the nonlinearity of a simple wave group, and examine the effects of the nonlinear waves on a moored floating breakwater. This is done by producing simple wave groups in a wave flume, and examining the output.

The laboratory tests were carried out in the wave flume at University of Padova in cooperation with Professor Luca Martinelli. The wave tests did not yield perfect results, as the exact generation of the desired waves was not possible. Though the desired waves were not generated, the results were considered to be suitable for the further analysis.

A model of a floating breakwater was installed with mooring system consisting of crossing chains. The chains were fitted with strain gauges in order to obtain the forces in the mooring lines during testing. The motions of the model were recorded by an optical motion detection system. The results of the laboratory testing are analysed in order to determine the Response Amplitude Operator (ROA) of the floating breakwater, giving an indication of the response of the model with respect to the energy content of the waves.

The RAO is found by determining the transfer function from the wave spectrum to the spectrum of the response for surge motions in the direction of the wave propagation, the pitch motions, rotations around the length axis of the model and for the forces occurring in the mooring lines.

The surge motions show indication of a nonlinear response, with a large response at low frequencies, while the response at the input frequencies of the spectrum for all tests is close to 1.0. This is in correspondence with what has previously been documented regarding the response in a grouped sea state, and clearly shows the nonlinear behaviour of the waves. The pitch motions were found to have a more linear response, going well along with the fact that the amplitude of the nonlinear waves are considered small.

The analysis of the forces in the mooring lines shows a nonlinear response as well. However, the result of the force analysis does not give good results due to the setup of the mooring system. The weight of the mooring lines is not enough to prevent snapping forces to occur, giving an unrealistic response of the forces.

The overall analyses of the performed tests shows the presence of a nonlinear response, of the floating construction. This indicates that it is relevant to consider the grouping of waves, when designing the mooring systems of floating constructions.

Summary in Danish

Ved at betragte naturlige bølger på havet, kan man til tider observere bølger sammensluttet i grupper. Når bølgegrupper dannes giver det anledning til dannelsen af ikke lineære bølger, som resultat af interaktion mellem bølger. Det har været observeret, at der som følge af dette ikke lineære fænomen, kan optræde ikke lineære flytninger af forankrede flydende konstruktioner. Disse flytninger kan give anledning til store kræfter i forankringssystemet, hvilket kan føre til brud.

I dette projekt er målsætningen at dokumentere tilstedeværelsen af ikke lineære bølger i en simpel bølgegruppe, og undersøge de deraf følgende effekter på en forankret flydende mole konstruktion. Dette er udført ved at generere simple bølgegrupper i et bølgeflume, og analysere resultaterne.

Laboratorieforsøgene er udført i bølgeflumet på University of Padova, i samarbejde med Professor Luca Martinelli. Forsøgene gav ikke de gode resultater, da det ikke var muligt at generere de ønskede bølger. De genererede bølger er dog vurderet som brugbare til brud ved den videre analyse.

Der blev udført forsøg med en model af den flydende mole, opsat med et forankrings system bestående af krydsende kæder. I kæderne blev der installeret Strain Gauges, for at måle kræfterne i forankringskæderne under bølgetest. Bevægelserne af modellen blev optaget med et optisk object detection system. Resultaterne af laboratorietest er analyseret for at bestemme Response Amplitude Operator, hvilket giver en indikation for modellens respons fra bølgenes energi spektrum.

ROA'en findes ved at bestemme en transfer funktion fra bølgenes energi spektrum til spektrummet fra responsen. Dette er udført for surge flytninger, pitch flytninger og kræfter i forankringskæderne.

Fra analysen af surge bevægelserne er der en indikation af et ikke lineært respons. Dette kommer til udtryk ved et højt respons fra lavere frekvenser, mens responset fra input frekvenserne er tæt på en for alle tests. Dette er i sammenhold med hvad der tidligere er blevet dokumenteret, ved analyse af respons fra gruppering af bølger. Fra analysen af pitch bevægelserne kommer et mere lineært respons til udtryk, hvilket stemmer overens med antagelsen om små amplituder ved anden ordens bølger.

Fra analysen af kræfterne i forankringskæderne er der et tydeligt ikke lineært respons. Resultaterne fra analysen af kræfterne er dog ikke fuldt ud brugbare, da der forekom snapping i kæderne under bølgetest, hvilket indikerer at mooring systemet ikke er designet optimalt. På grund af snapping bliver responset urealistisk højt.

Overordnet viser analysen af de udførte tests et ikke lineært respons fra den flydende mole. Dette indikerer at det er relevant at tage forekomsten af bølgegrupper med i betragtning, ved design af forankrings systemer til flydende konstruktioner.

Table of Contents

I Main Report	1
1 Introduction	3
1.1 Wave Grouping	3
1.2 Nonlinear Effects	4
1.3 Problem description	5
2 Preparation of Laboratory Testing	7
2.1 Wave Generation	7
2.2 Estimation of Output	9
3 Motion Detection of Breakwater	17
3.1 Motion Detection Method	17
3.2 Object Detection	18
4 Wave Testing	19
4.1 Flume Layout	19
4.2 Analysis	22
5 Test Setup	29
5.1 Test subject	29
5.2 Mooring Systems	30
6 Analysis of Test Results	33
6.1 Movements of Breakwater	33
6.2 Forces in Mooring Lines	39
7 Discussion	45
8 Conclusion	49
References	51
II Appendix Report	53
A Object Detection	55
B Wave testing	57
B.1 Waves	57
C Analysis of aquisition rate	61
C.1 Installing strain gauges	61
D Analysis of movements	63

Part I

Main Report

1 Introduction

In this project the response of a moored floating structure subjected to nonlinear waves is investigated. This is done primarily by performing model tests in a wave flume.

In recent years the offshore and coastal zones have set the scene for an increasing activity in the use of floating structures, spreading across various sectors of industry from offshore oilrigs, wind turbines and energy converters to the use of floating breakwaters and coastal protection systems. The mooring systems vary in design from taut lines and tension leg platforms to constructions moored with mooring lines or chains. It has been observed that the movements and forces occurring in the mooring systems are larger than expected for the sea states in a given region. This has been shown to be related to effects occurring in grouping of waves. It has been documented that interaction between two waves in a wave group gives a nonlinear response in the form of second order wave components. When a floating structure is moored in a multi-frequency wave field, it will be excited to second order wave forces, deriving from this interaction between harmonic wave trains travelling in the same direction. [Fonseca *et al.*, 2011]

1.1 Wave Grouping

In nature when short period waves are generated during a storm, they are usually considered as a completely irregular sea state, which can be described by a spectrum such as the JONSWAP spectrum. However, in some cases a correlation is observed, making the waves travel in groups propagating with the group velocity. Wave groups can be recognized as distinct sequences of high waves in an irregular sea state. The groups are formed by the summation of a number of regular waves. The waves can be heavily grouped or lightly grouped, described by a grouping factor GF [Sand, 1982b]. In figure 1.1 an irregular non grouped sea state is shown, and in figure 1.2 a highly grouped sea state can be seen.

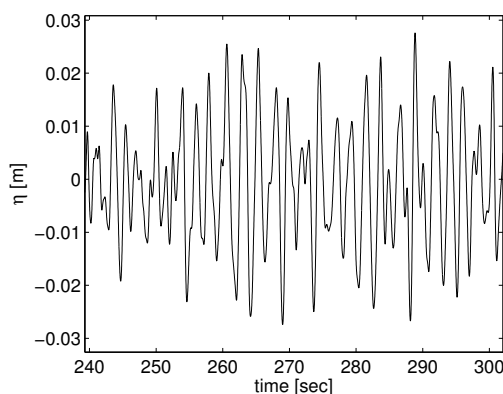


Figure 1.1. Irregular sea state.

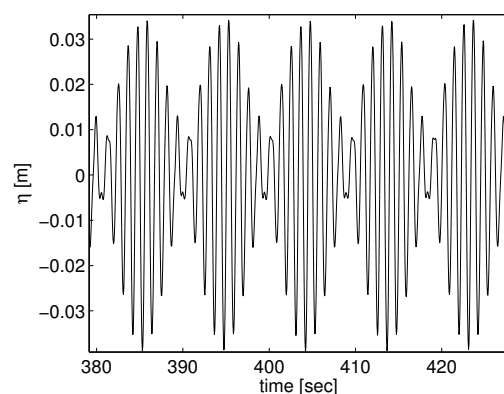


Figure 1.2. Highly grouped sea state.

1.2 Nonlinear Effects

In many cases the linear wave theory gives good results, but it becomes relevant to look at the nonlinearity of the waves, in the cases where the neglected nonlinear part starts having an influence. The most widely known nonlinear theory is Stokes second order theory. It is derived by the perturbation method, meaning that it is solved by starting from a known exact solution, in this case the linear wave theory. The second order term is then added to the linear solution in order to obtain the second order solution. [Svendsen, 2006] This can be considered as taking a regular sine wave from linear wave theory, and adding the second order term in form of a higher harmonic wave. The higher harmonic wave was by Stokes shown to be a bound wave with double frequency, traveling with a celerity determined by the primary wave. The second order part steepens the wave, making a sharper crest and a flatter trough. [Sand and Mansard, 1986]

Wave to Wave Interaction

As mentioned above, a natural wave train can be composed of waves at several frequencies. If a simple case of only 2 frequencies forming a wave group is considered, the linear description of the two waves can be extended to show that the grouping of the waves will create two additional waves. The two waves will be of second order.

The second order components can be divided into subharmonics and superharmonics. The subharmonics being in the form of a bound long wave, with a frequency equal to the frequency difference of the interacting waves. The superharmonics being short waves, with double frequency of the first primary wave, double frequency of the second primary wave and the sum of frequency from the primary waves. [Andersen and Frigaard, 2012]

The long waves in groups of regular waves, were by Longuet-Higgins and Stewart [1964] shown to occur due to radiation stresses. Later studies by Hansen [1978] of applying the momentum equation to irregular wave trains, has shown that the long waves are of second order, and the amplitudes are proportional to the squared amplitudes of the primary waves. The long wave is bound to the two waves from which it originate, and is by such not dispersive. The properties of the long waves is determined by the frequencies and wave numbers from the primary waves. An example of a spectrum including the second order waves is shown in figure 1.3.

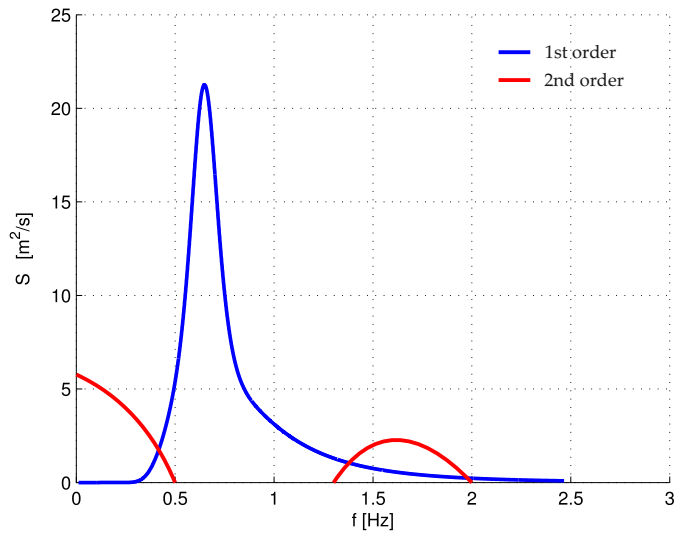


Figure 1.3. Spectrum containing both first order and second order waves.[Andersen and Frigaard, 2012]

1.3 Problem description

Moored constructions often have a long natural period of oscillation, giving an Eigenfrequency often well below that of the waves. However, the long waves generated by wave to wave interaction could have a frequency close to that of the moored construction. The aim of this project is to experimentally document the effect of the second order long waves on the mooring forces and slow-drift oscillations, for a moored floating construction. This is sought to be done by creating resonance condition with incoming long waves. As the resonance of the system would be affected by any damping induced to the system, a non disturbing method will have to be developed, to measure the motions of the floating construction.

2 Preparation of Laboratory Testing

In this chapter the preparations prior to doing the laboratory testing is presented. In order to do successful wave testing, the theory of producing the correct waves is presented to ensure the correct waves are produced. The theory of second order waves will then be used to produce initial predictions of the generated waves. The predictions will include first and second order waves plus an estimate of the reflected waves.

2.1 Wave Generation

In order to determine the effects of the long waves on a moored construction, a model of a floating breakwater moored with crossing chains is chosen as the test model. As the long waves in a wave group occur from the interaction between every regular wave in the group, an irregular wave spectrum would produce a large number of long waves. Due to this, it is difficult to separate the effect of the long waves. To determine the effect of one long wave, the simplest case of producing a long wave is chosen by producing a spectrum containing only two regular waves, which can be seen on figure 2.1. The second order waves which are produced are the double frequency waves, equal to the stokes second order waves, the sum of frequency wave and the frequency difference wave or the long wave.

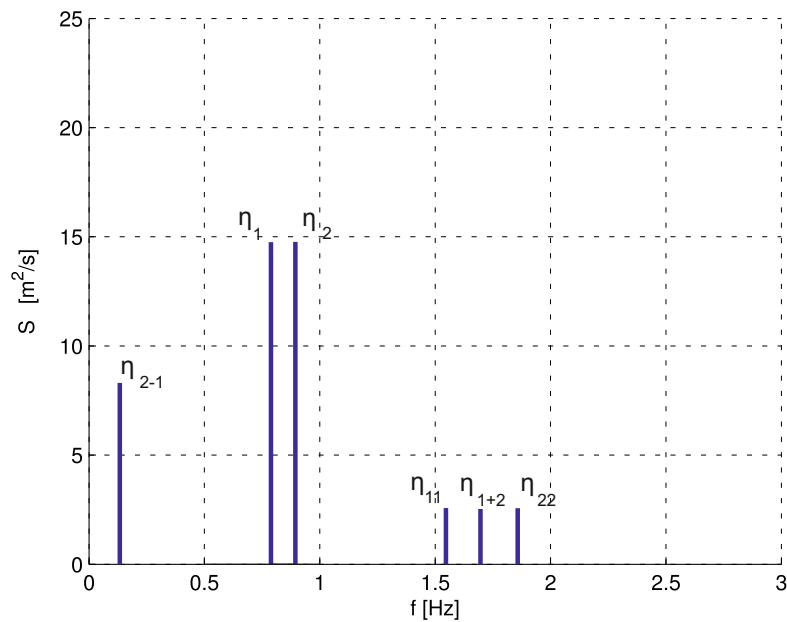


Figure 2.1. Spectrum used for wave testing.

2.1.1 Wave Tests

The monochromatic waves are chosen with a frequency difference of 0.1 Hz in order to get a long wave with a period of 10 seconds. This will generate a resonance condition with the model of the floating breakwater, which will be further described in chapter 5. For the testing, four pairs of monochromatic waves are chosen, which with the corresponding bichromatic waves gives a total of 12 tests to perform.

Table 2.1. Wave tests.

Test nr.	F_1 [Hz]	F_2 [Hz]	H_s [m]	E
1	0.8	-	0.03	0.0005
2	0.9	-	0.03	0.0005
3	0.8	0.9	0.04	0.0005
4	0.8	-	0.04	0.0010
5	0.9	-	0.04	0.0010
6	0.8	0.9	0.06	0.0010
7	0.8	-	0.06	0.0020
8	0.9	-	0.06	0.0020
9	0.8	0.9	0.08	0.0020
10	0.8	-	0.08	0.0040
11	0.9	-	0.08	0.0040
12	0.8	0.9	0.11	0.0040

2.1.2 Reproduction of Long Waves

As described in 1 - *Introduction*, the grouping of waves generates a series of bound subharmonics and superharmonics traveling with the group. This gives rise to some problems, when reproducing the natural irregular sea state in a laboratory. The bound sub- and superharmonics are of second order and normal orbital particle velocities called drift velocities. When using a first order control signal for the wavepaddle, as the Biesel transfer function, only the first order waves are generated. The orbital velocities related to the sub- and superharmonics are not generated. As there is there is no flow through the paddle, the lack of the second order harmonics is compensated by the creation of both the bound second order waves and free waves, or parasitic waves. [Hansen *et al.*, 1980]

The free waves have opposite phase of the bound waves, resulting in elimination of the orbital velocities at the paddle, and thus satisfying the boundary conditions of the first order wave generation. The free waves are not bound to the primary waves but follow the dispersion relationship. This can lead to an unrealistic response when performing laboratory testing, as the as the free and the bound wave will interact.

The solving of this problem has been the topic of several studies, in order to correctly reproduce the second order waves. The studies of Hansen *et al.* [1980] and Sand [1982a] derive methods for correct reproduction of the long second order waves, but ignore the superharmonics. The work of Sand and Mansard [1986] presents a method to correctly produce both subharmonics and superharmonics.

For this project the transfer function derived by Bredmose *et al.* [2005] is used for the wave generation.

$$G_{n,m} = \frac{\delta_{n,m}}{g} \left((\omega_n + \omega_m) \frac{H_{n,m}}{D_{n,m}} - L_{n,m} \right) \quad (2.1)$$

Where (2.2)

$$\delta_{n,m} = \begin{cases} \frac{1}{2} & \text{for } \mathbf{k}_n = \mathbf{k}_m, \\ 1, & \text{otherwise,} \end{cases} \quad (2.3)$$

$$H_{n,m} = (\omega_n + \omega_m) \left(\omega_n \omega_m - \frac{g^2 \mathbf{k}_n \mathbf{k}_m}{\omega_n \omega_m} \right) + \frac{1}{2} (\omega_n^3 + \omega_m^3) - \frac{g^2}{2} \left(\frac{\mathbf{k}_n^2}{\omega_n} + \frac{\mathbf{k}_m^2}{\omega_m} \right) \quad (2.4)$$

$$D_{n,m} = g K_{nm} \tanh(K_{nm} h) - (\omega_n + \omega_m)^2 \quad (2.5)$$

$$K_{nm} = |\mathbf{k}_n + \mathbf{k}_m| \quad (2.6)$$

$$L_{n,m} = \frac{1}{2} \left(\frac{g^2 \mathbf{k}_n \mathbf{k}_m}{\omega_n \omega_m} - \omega_n \omega_m - (\omega_n^2 \omega_m^2) \right) \quad (2.7)$$

ω | Angular frequency of wave
 \mathbf{k} | Wave number

Absorbion of Long Waves

Long waves will typically cause problems during model tests, as they are very difficult to absorb and will cause reflection in the flume. This can be avoided by absorbing the short period waves as spilling breakers on a mild slope. In this way the energy from the long wave will also be dissipated. It is not possible to completely absorb the waves, why active absorption is used at the wave generator. The absorption system consists of two wave gauges at the paddle, finding the average surface elevation at the paddle. The part of the surface elevation that is considered a wave that will be reflected, is then used to alter the control signal sent to the paddle.

2.2 Estimation of Output

In order to get an estimate of the waves that will be generated, the notation by Bredmose *et al.* [2005] described above, is used to calculate the surface elevations in the flume, when inputting the primary waves. This will be used to compare the actually generated waves, with the theoretically expected waves. The output is a time series of surface elevations at the wave gauges. This is used for comparison with the surface elevations during testing. The surface elevations are calculated for the first row of gauges.

By solving the wavefield on matrix form, the transfer function as shown in equation 2.1, outputs the sum of the surface elevation for all four bound components.

$$\eta^{(2)} = \eta_{nm}^{(2)} + \eta_{mm}^{(2)} + \eta_{nn}^{(2)} + \eta_{n-m}^{(2)} + c.c \quad (2.8)$$

$$\eta_{nm}^{(2)} = \frac{1}{2} G_{n,m} A_n A_m e^{i(\theta_n + \theta_m)} \quad (2.9)$$

$$\eta_{mm}^{(2)} = \frac{1}{2} G_{m,m} A_m A_m e^{2i\theta_m} \quad (2.10)$$

$$\eta_{nn}^{(2)} = \frac{1}{2} G_{n,n} A_n A_n e^{2i\theta_n} \quad (2.11)$$

$$\eta_{n-m}^{(2)} = \frac{1}{2} G_{n,-m} A_n A_{-m} e^{i(\theta_n - \theta_m)} \quad (2.12)$$

The input to the program are,

- Flume dimensions - length, water depth, placement of wave gauges, reflection coefficient.
- Wave input - waveheight, frequency.

The output wanted is the primary and secondary wavefields, plus the reflection of the primary waves. The primary wavefield is found by equation 2.13,

$$\eta^{(1)} = \frac{1}{2} A_n e^{i\theta_n} + \frac{1}{2} A_m e^{i\theta_m} + c.c \quad (2.13)$$

2.2.1 Output

In this section the output surface elevations for test 7 and 9 will be presented. Only test 7 and 9 are shown, as test 8 is identical to test 7, besides the difference in frequency. Throughout the report the results from tests 7-9 are presented, the results for the remaining tests can be found in the appendix.

Test 7

In test 7 a monochromatic wave with a wave height of 0.06 meter and a frequency of 0.8 Hz is generated. The wave is composed of a linear wave and a second order component at double frequency. A short sequence of the surface elevation is shown in figure 2.2.

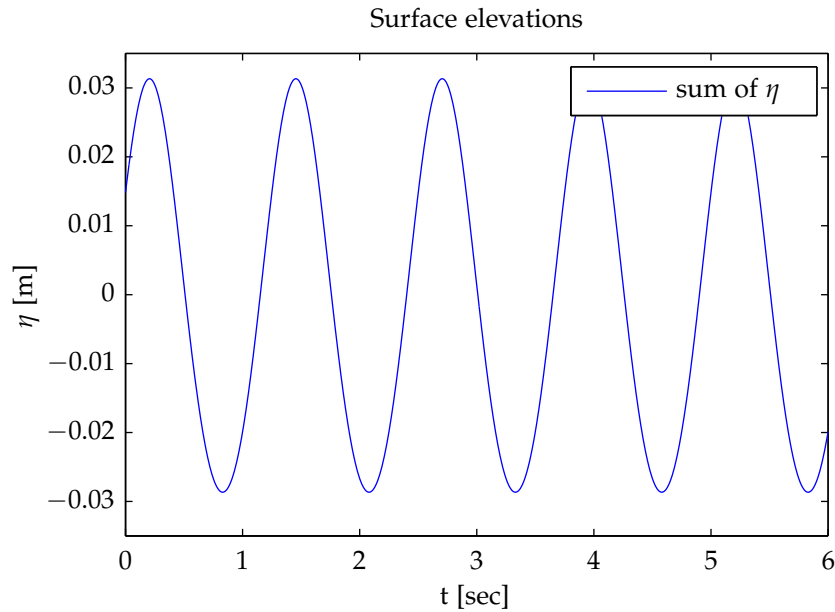


Figure 2.2. Surface elevation at the first row of gauges, test 7.

In figure 2.3 the first order wave is plotted together with the sum of the first and second order. It can be seen that in accordance with Stokes second order wave theory, the second order wave is steeper with a higher crest and a smoother trough.

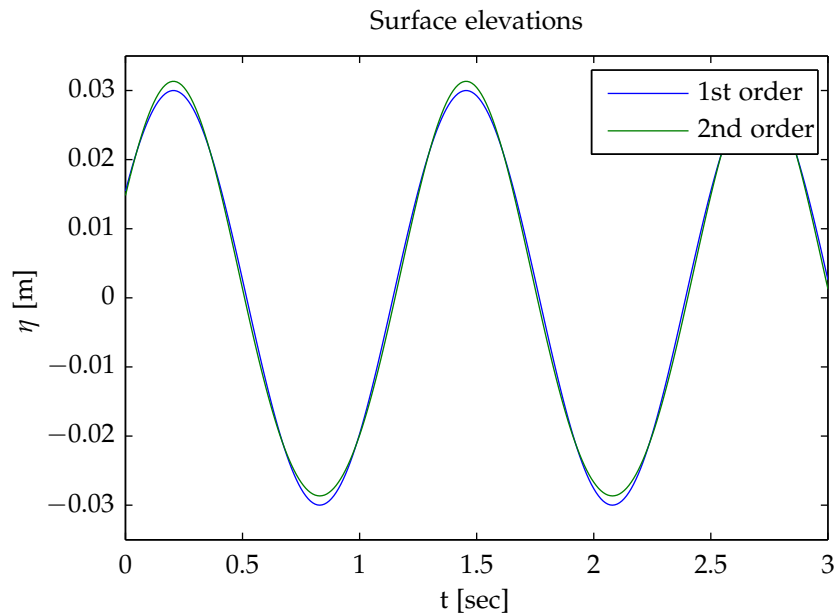


Figure 2.3. First order and second order waves, test 7.

Test 9

The wave in test 9 is the sum of the waves in test 7 and 8. The primary waves have a wave height of 0.06 meter and frequencies at 0.8 and 0.9 Hz. On figure 2.4 a sequence of the surface elevation of test 9 can be seen. It can be seen that the waves form wave groups with a group period of 10 seconds, corresponding to the 0.1 Hz frequency difference of the primary waves.

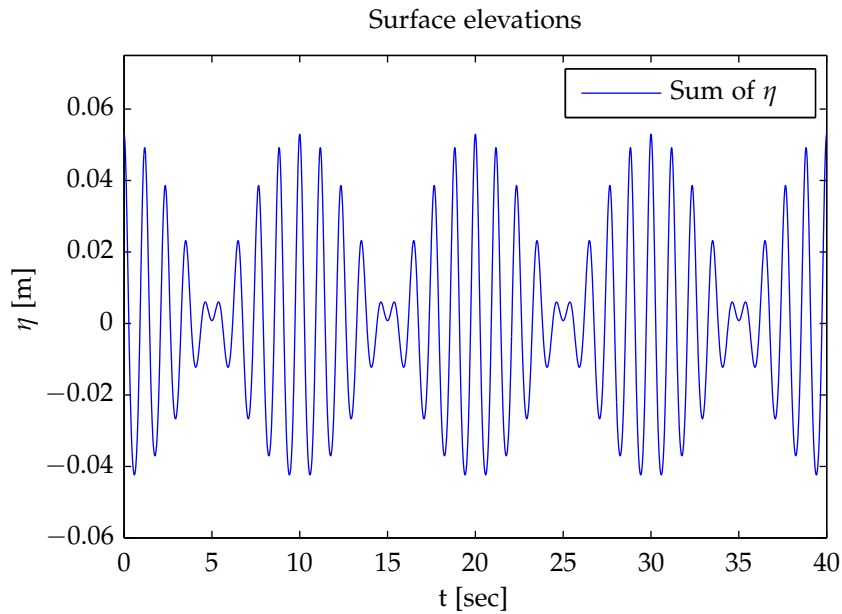


Figure 2.4. Surface elevation at the first row of gauges, test 9.

The summation of the two first order waves can be seen plotted together with the sum of the first and second order waves in figure 2.5

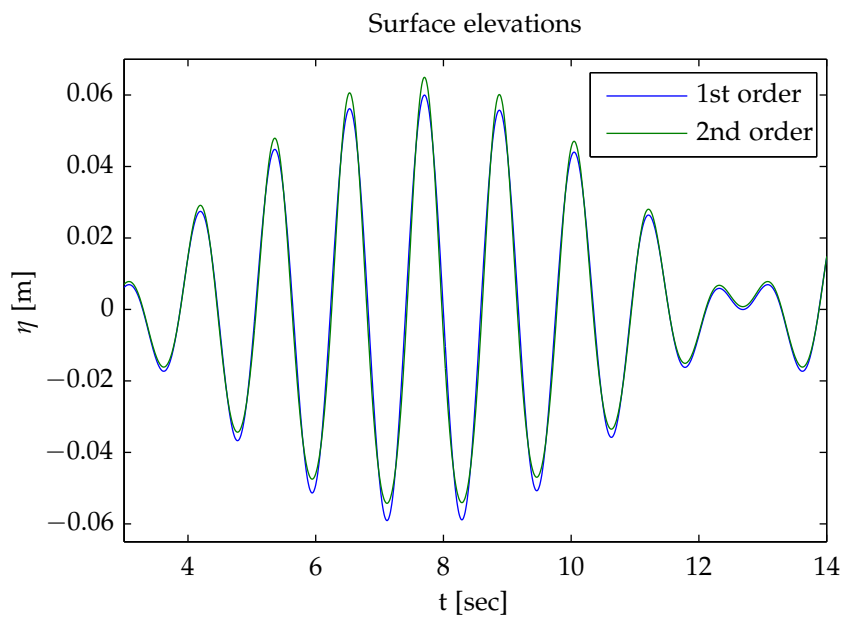


Figure 2.5. First order and second order waves, test 9.

The long wave component is a relatively small amplitude wave compared to the primary waves. In figure 2.6 the surface elevation can be seen together with the scaled amplitude of the long wave. It can be seen that the long wave produces a setdown at the sum of the primary surface elevations, and increases the wave height, when the primary waves cancel each other.

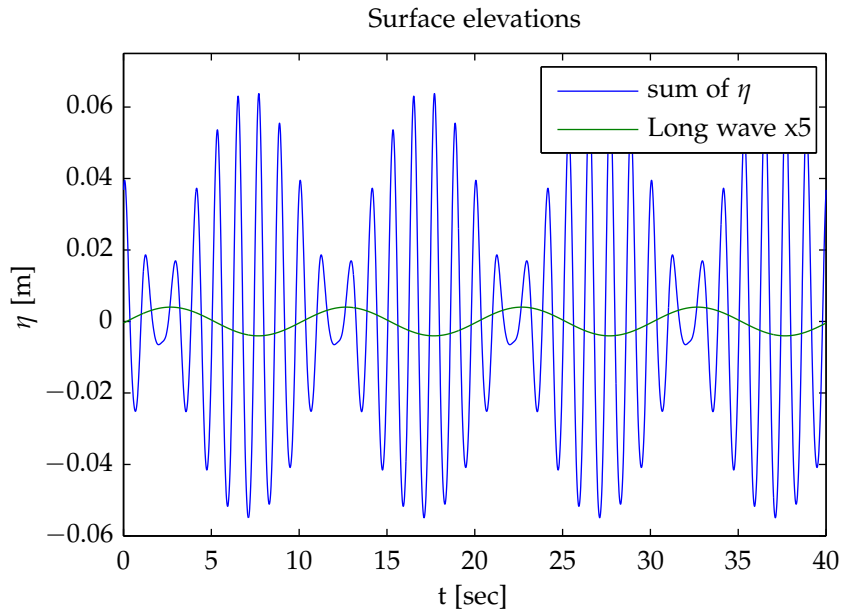


Figure 2.6. Surface elevation and long wave component for test 9.

As explained above, the long waves are difficult to absorb in laboratory testing. In figure 2.7 the surface elevation along the flume at an instant, can be seen. The waves are relatively short and are expected to break when the bottom of the flume starts to slope.

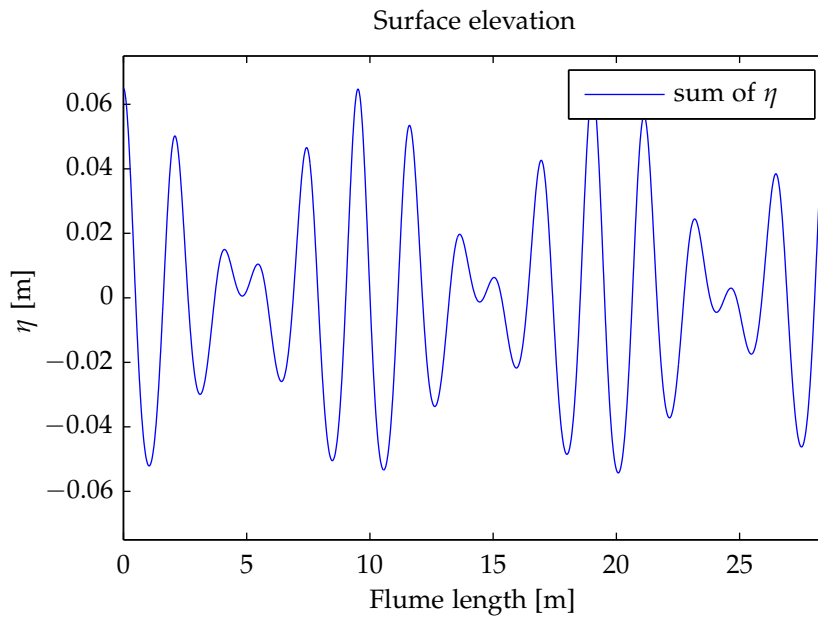


Figure 2.7. Surface elevation along flume for 9.

The surface elevation due to the long wave along the flume can be seen in figure 2.8. It can be seen that the long waves have a length close to 10 meters, making them very difficult to absorb when using a gravel beach or absorbing mat.

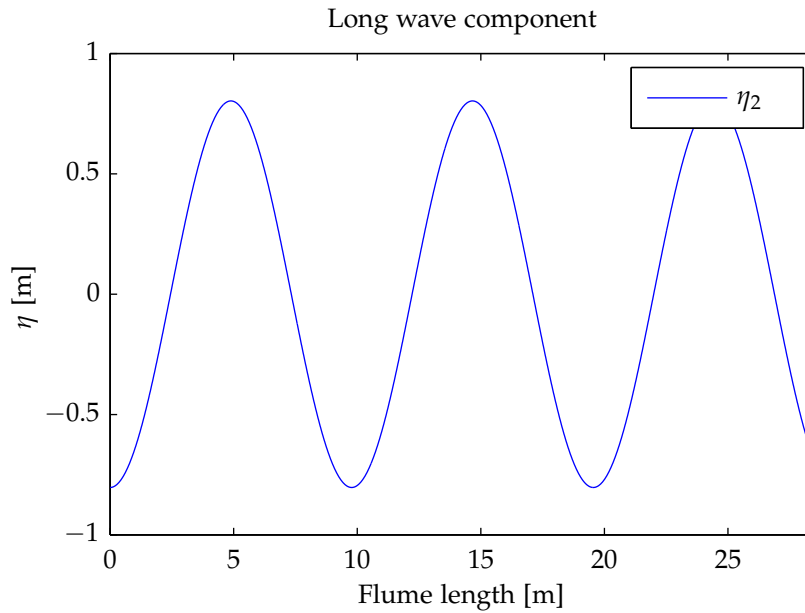


Figure 2.8. Surface elevation from long wave along flume.

2.2.2 Analysis

As the aim of the laboratory testing is to determine the effect of the long wave on the floating breakwater, it is natural to analyze the movements of the breakwater in frequency domain. In order to have comparative results from the initial calculations, the same approach will be used here. The output is analyzed by finding the Power Spectral Density or PSD. The PSD gives an estimate of the amount of power per frequency interval. The PSD is found by dividing the time signal into sequences, and finding the Fourier transform of every time sequence. The magnitudes of the Fourier transforms are squared and divided by the length of the time sequence. The resulting series of transforms from the time sequences are the averaged in order to obtain the average power per frequency interval. It is clear the averaging influences the reliability of the output. If the initial signal is split into longer sequences, the resulting variance of the PSD is smaller. When calculating the PSD, the *pwelch* function is used. The function finds the Welch's spectral density estimate, by overlapping the time sequences by a given percentage of the length of the sequence. The sequences are then windowed before finding the Fourier transform.

Test 7

The PSD of the surface elevation from test 7 can be seen in figure 2.9 and 2.10. The PSD is calculated for a 100 second signal, where sequences of 100 and of 10 seconds are used. It can be seen that the PSD calculated for one sequence equal to the entire signal, is spikier and clearly separates the frequency intervals containing the energy. The PSD calculated from sequences of 10 seconds is wider and clearly has a larger variance. However, both figures show a clear presence of power around the frequencies 0.8 and 1.6 Hz, equivalent to the frequencies of the primary and secondary wave.

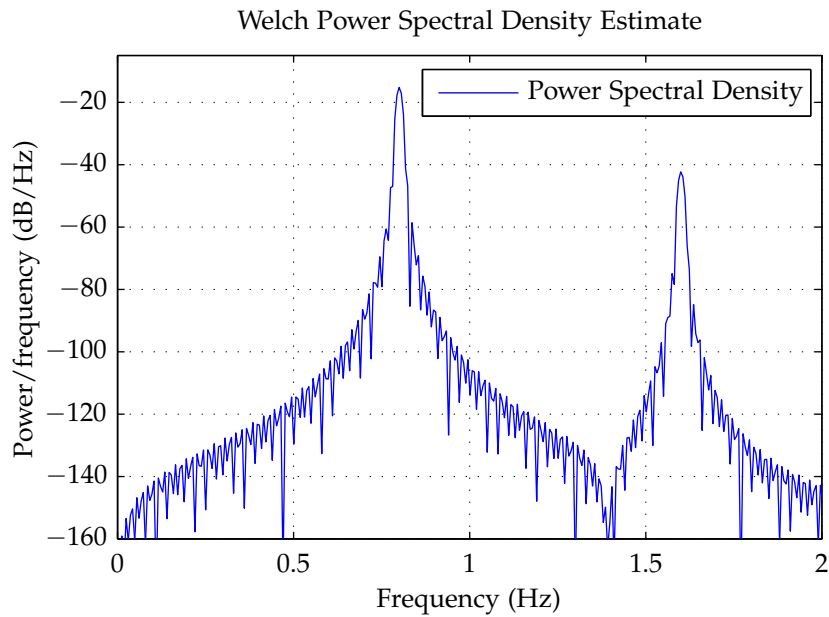


Figure 2.9. PSD with 100s window of time series from Test 7 front wave gauges.

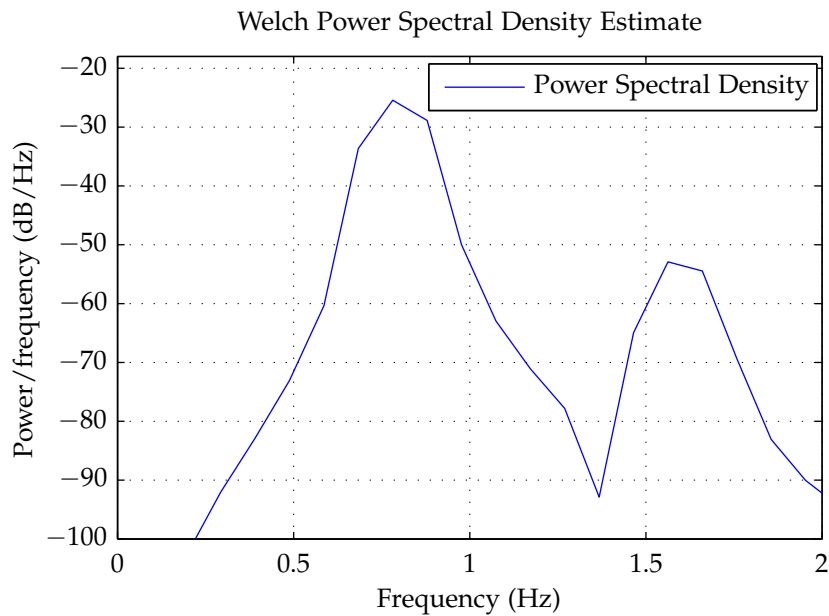


Figure 2.10. PSD with 10s window of time series from Test 7 front wave gauges.

Test 9

The PSD of the surface elevation from test 9 can be seen in figure 2.11 and 2.12. There is a clear presence of energy at the two primary frequencies, 0.8 and 0.9 Hz. The energy from the long wave can be identified at a frequency of 0.1. There are three high frequency peaks, at 1.6, 1.7 and 1.8 Hz. This corresponds with the higher harmonics at double frequency and sum of frequency.

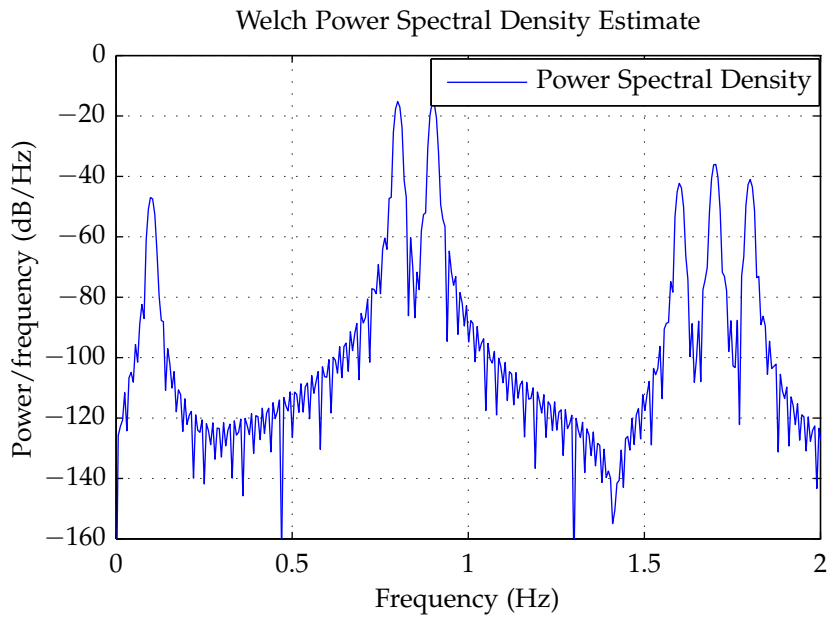


Figure 2.11. PSD with 100s window of time series from Test 9 front wave gauges.

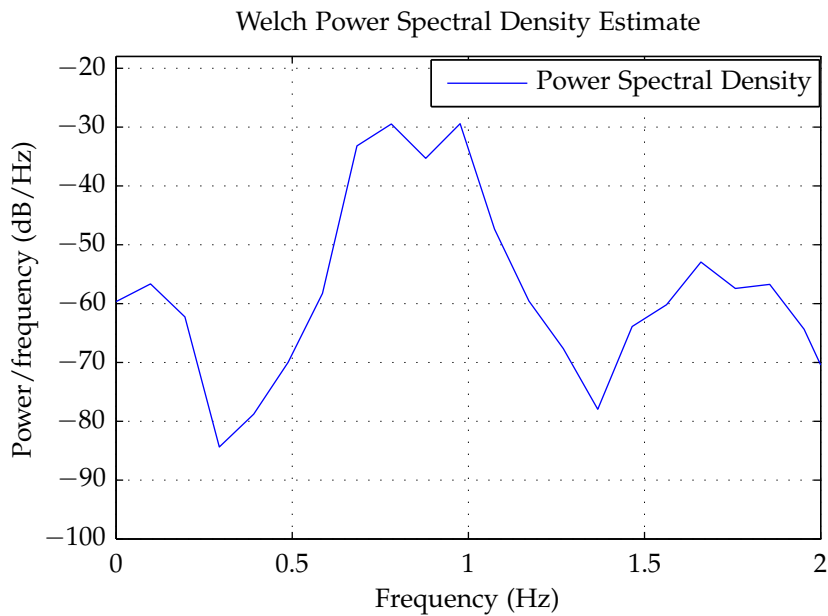


Figure 2.12. PSD with 10s window of time series from Test 9 front wave gauges.

Conclusions

The second order wave components can only be correctly reproduced by using a second order transfer function for wave generation. The second order transfer function was used to calculate the amplitudes, frequencies and wave numbers for the second order waves. This was used to produce estimates of time series of the surface elevation in the flume. From time series the PSD were calculated, in order to produce the power spectrum for correct first and second order waves. This can then be used to ensure that the correct waves are produced in the laboratory testing.

3 Motion Detection of Breakwater

The movements of the breakwater caused by second order waves are considered to be a very small part of the total movements. Due to this, there is a very small tolerance for the motion detection systems influence on the breakwaters movements. Furthermore the movements are fitted to occur due to resonance with the mooring system, why any damping on the system will disturb the movements. In this chapter the choice and use of motion detection system will be discussed.

3.1 Motion Detection Method

The motions of the breakwater should be detected in order to determine the influence of the second order waves. In order to do so, several types of motion detection methods could be used. The available methods for motion detection for this project are the use of movement gauges, installing accelerometers and gyros on the breakwater and doing video recording of the movements. The use of each method is evaluated, in order to choose the best method for the specific task.

Movement Gauges

The movement gauges consists of a line on a roll, connected to a spring. The movements of the line are digitally recorded with good precision, and the spring ensures the line is always tight and will go back to zero. The advances of using the movement gauges are that they are easy to install without having to alter the setup. The data tracking is directly available as a measure from the movement gauges, which reduces the post processing time of the data. The disadvantages of the movement gauges are that the gauge exerts a elastic force of 1.0 Newton on the breakwater, causing it to deflect from the zero position. Further and more critical the spring acts as a damper on the breakwater, which will damp out the effects of the resonance that is investigated.

Accelerometer and Gyro

The motions of the breakwater could be recorded by installing a series of accelerators and gyros, which would make it possible to determine the velocities and the position. The advantages of using this system are that there are limited external effects influencing the motions of the breakwater, giving a better chance to observe the desired effects. If installed correctly the system could be very precise. The disadvantages are that the installation and interpreting of results could be very complicated and be a source of errors. When going from accelerations to displacement, there could occur a drift that would have to be taken into account.

Video Recording and Object Detection

The motion detection system of the breakwater could be made by video recording the movements of the breakwater during testing. The post processing would consist of performing object detection on the video recordings, and by so track the movements of the breakwater. The advantage of this method is that no gauges would be installed on the breakwater, besides the strain gauges measuring the forces in the mooring lines. It is easy to perform as the test can be run without acquiring data from any gauges. The

disadvantages are the post processing, as motion tracking systems would have to be developed. The reliability and accuracy of the system could be an issue.

Choice of Method

As the movement gauges induces a large damping on the system, it is the least favorable method, and thus the choice was between the accelerometers and video recording. The method of video recording was chosen, due to the possible problems that might be encountered by using accelerometers and gyros.

3.2 Object Detection

Digital object detection on video recordings is a very well developed but complex subject, and could be a research topic in it self. Due to this, the emphasis was on simplicity and well known methods, when developing the object detection system for this project.

For this project a simple method of identifying objects based on their RGB color is used. An example of object detection by this method can be seen in Appendix A - *Object Detection*. When using this method, where everything besides the pixels with pixels with a high red value on the RGB scale is removed, any other objects in the picture with high red components will interfere and complicate the tracking process. This is a problem as white light is composed by the maximum value in the red, green and blue. Due to this, minimizing the amount of light in the room will lower the amount of disturbance, from light being reflected by glass or metal. By lowering the light it becomes harder to track a regular object, making it favorable to track a small moving light source like a laser dot.

It was chosen to install two white LEDs on the breakwater for tracking. Laser dots would have been the best solution, as they give a more concentrated emission of light, and by so reduce the disturbance. It was however not possible to install the laser pointers, why the LEDs where chosen. As described above, white light consists of the maximum value of red, green and blue, and by so searching for red objects will still output the white LEDs.

The tracking of the diodes is done by using the method described above and with frame by frame recognizing the two objects. The objects are assigned an area, defined by the number of pixels they consist of, and a centre point defined by the center of mass of this area. For every frame, the coordinates in pixels for the center of mass is extracted, and stored as separate time series of coordinates for LED no. 1 and 2. As the distance between the diodes is known, the pixel coordinates can be transferred into coordinates in meters. For the testing a video camera recording at 25 frames per second was used giving a sampling rate of 25 Hz. This is considered a reasonable sampling rate for the desired motion detection.

4 Wave Testing

To ensure the correct waves are generated, the waves are tested before inserting the floating breakwater. As described in 2 - *Preparation of Laboratory Testing*, the aim is to produce a summation of two regular waves. In order to analyze each component, it is wanted to produce each regular wave separately in tests, and then run a test with the summation.

4.1 Flume Layout

The tests are performed in the 36 meter long wave flume at the University of Padova. The waves are generated by a piston type wavemaker, with two wave gauges mounted for active near field absorption. The water depth used for testing is 0.85 meter at the paddle and 0.8 meter at the position of the breakwater. After the position of the breakwater the water depth decreases with a slope of 1:10 for 4 meters before going into a gentle slope leading up to an absorbing mattress. The flume layout can be seen of figure 4.1.

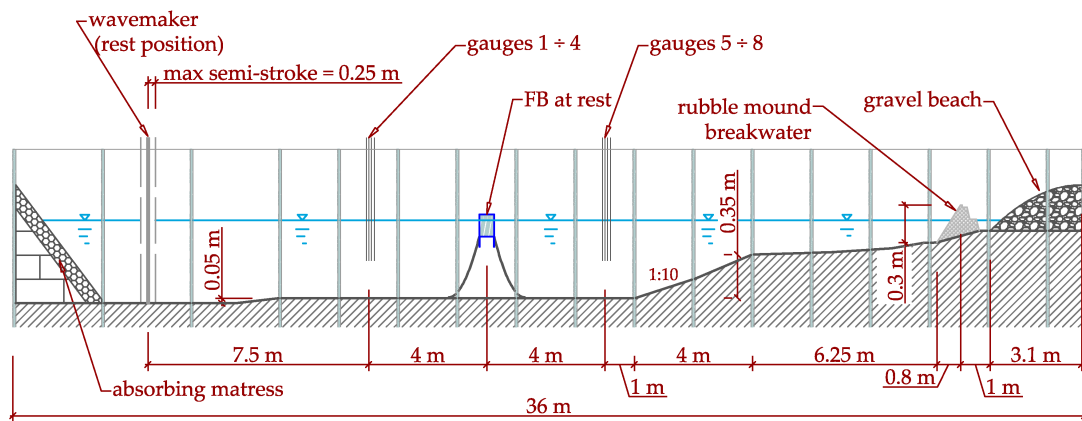


Figure 4.1. Layout of flume. [Pezzutto, 2013]

The tests are performed in a flume by HR Wallingford, and the wave generator is controlled by the program *HR Wavemaker Wave generation control program*. When using this program, the only option to produce the desired waves is to use white noise filtering and defining a custom wave spectrum. A number of problems is encountered when using this method. Firstly the HR Wavemaker scales down the custom spectrum to 24 frequency steps, based on the input on the 8th frequency slot. This limits the frequency discretization to 24 slot, and a starting frequency of 0.1Hz. The second problem is that when using white noise filtering for long time series, even a spectrum only containing energy in one frequency step will look like a random sea state. This can be seen on figure 4.2, where a section of a 600 second test sequence is shown.

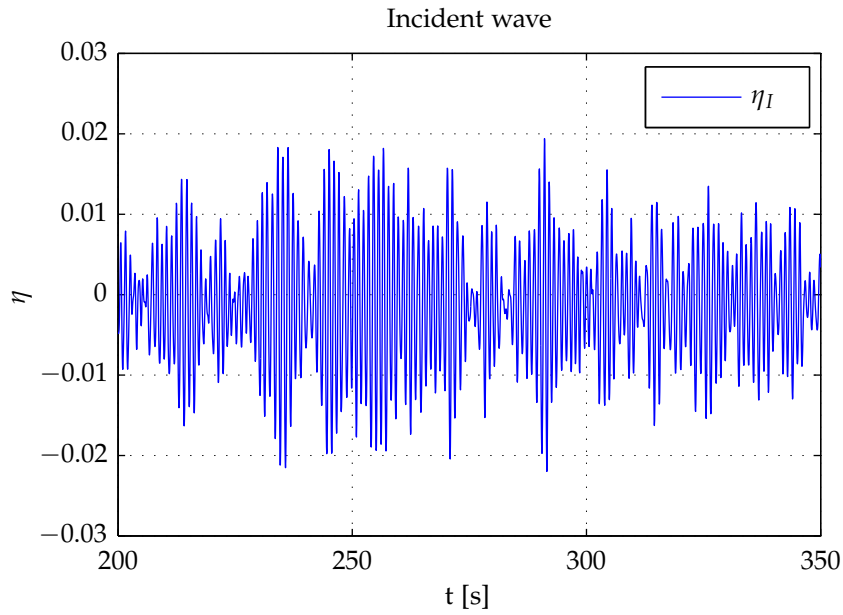


Figure 4.2. Generated waves at long running sequence.

In order to avoid generating a random sea state, and produce the desired signal consisting of a regular wave, the run time was lowered to 10 seconds. A test of 600 seconds would then consist of 60 sequences of 10 seconds. To ensure the same signal would be generated for every sequence, the starting sequence was fixed for the white noise filtering. This still gives a varying sea state within the 10 seconds, but the total signal is periodic. On figure 4.3 and 4.4 sections of the repeated signal can be seen, for a wave with a frequency of 0.8Hz one with 0.9Hz.

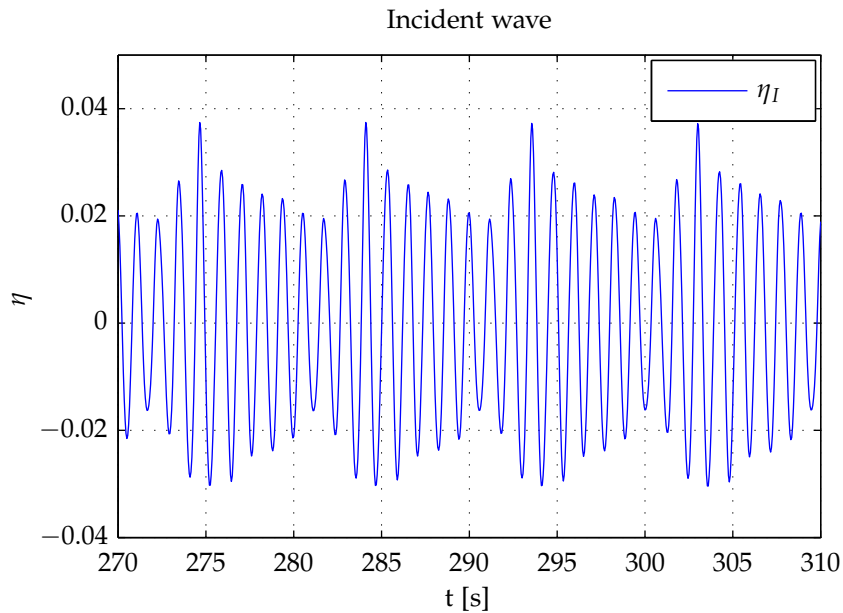


Figure 4.3. Test 7 generated waves.

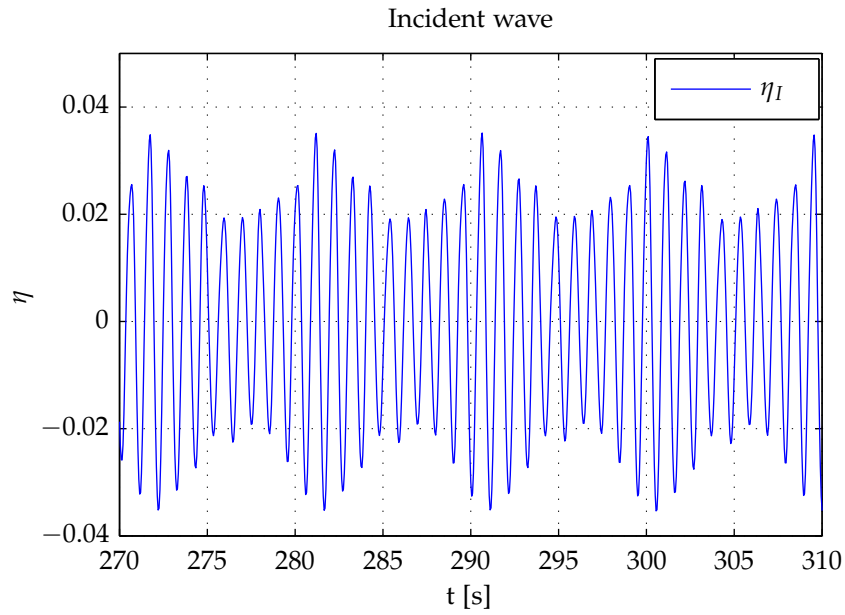


Figure 4.4. Test 8 generated waves.

As it can be seen the generated waves are not regular, but more resembles summations of two waves. This might induce some errors when analyzing the waves, such as it might include energy at the low frequencies, which was exactly what was sought to be avoided, as it will make the results less clear in the combination of the waves. However, the waves are the closest to desired waves that the wavemaker can produce, so they will be used for the further analysis. On figure 4.5 the summation of the waves on figure 4.3 and 4.4 can be seen. It is clear that even though the regular waves where not perfect, the summation of the two waves is very close to the desired wave.

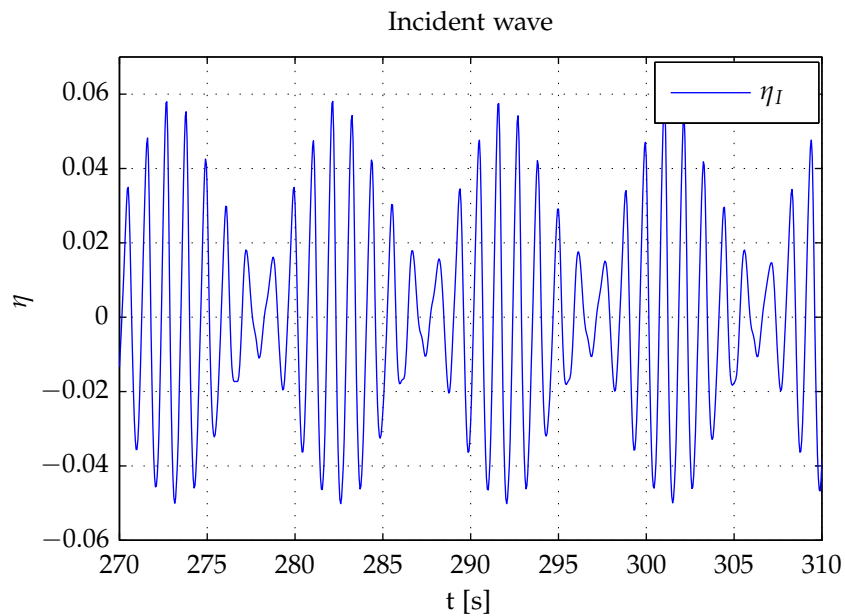


Figure 4.5. Test 9 generated waves.

4.2 Analysis

When using the PSD function in MATLAB, the data is windowed in order to smoothen the output, as described in chapter 2 - *Preparation of Laboratory Testing*. An overlapping of 50 % and windowing by a Hann window is chosen. The segment length for each window has great influence on the output signal. A large window will give a rippled spectrum, with a more exact representation of the spreading, while a smaller window will give a smooth spectrum. When using the window, the data is fitted to the window, which induces some error. When as in this case the windows are relatively small, the data gets a false periodicity from the arc formed window. This could be reduced by using a squarer window, but this would create a number of large frequencies in the signal. To reduce the effect of the window on the low frequencies, a large overlapping of the windows is used.

The window size, or the amount of data points per window, is found by finding the segment length of the signal, where the signal repeats and overlaps. This is done by creating an $n \times m$ zero matrix, where n is the initial estimate of the sequence length, and m is an arbitrary number sufficiently large so that $n \times m$ is larger than the length of the signal. Now column by column the data is inserted into the matrix. Then the sequence length n can be found by iteration, by finding the length producing the smallest standard deviation of the matrix. The theoretical window should be 200 points, as the sampling rate is 20 and the waves are repeated every 10 seconds. This is however not the case, probably due to inaccurate generation of the waves. The actual window is 189 points, on figure 4.6 the plot of the matrix can be seen for this sequence length. It is clear that the signal repeats itself, and this is a proper window length for the spectrum.

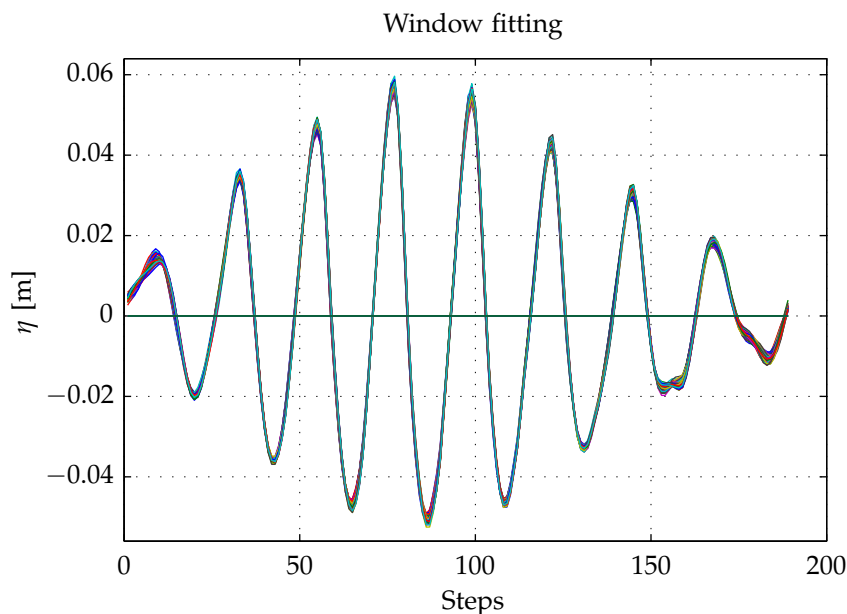


Figure 4.6. Plot of the sequences used for windowing the data, test 7, 8 and 9.

Test 7

The PSD of the surface elevations from test 7 is calculated and plotted on figure 4.7 with one window containing the full signal and 4.8 using a window length equivalent to the segment length determined above. The spectrum shows a clear presence of energy near

0.8 Hz and 1.6 Hz, corresponding to the first and second order waves. The PSD from the full window shows peaks in the energy on wide range of frequencies, this can perhaps be explained by the presence of reflected waves and higher frequency waves formed by breaking at the boulders. Some of the peaks might also be explained by a not complete periodicity of the waves.

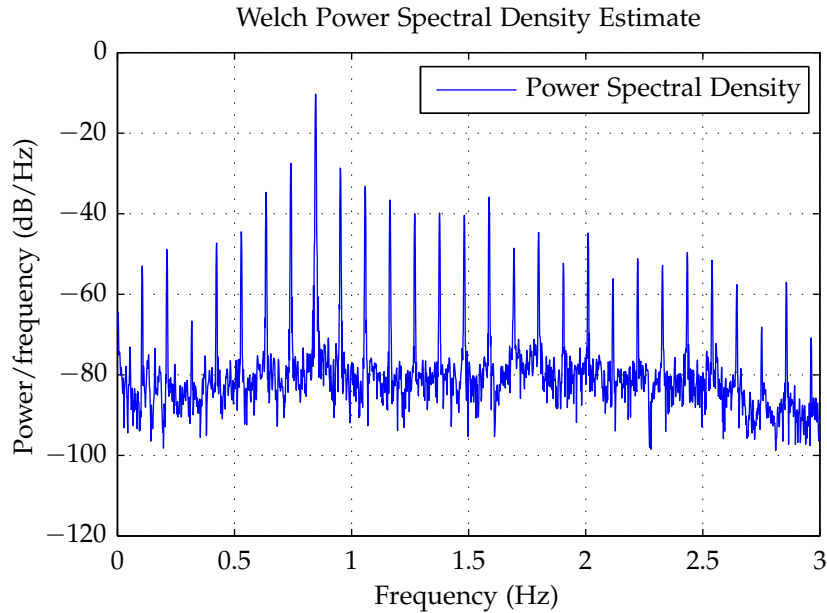


Figure 4.7. PSD of test 7 with large hanning window.

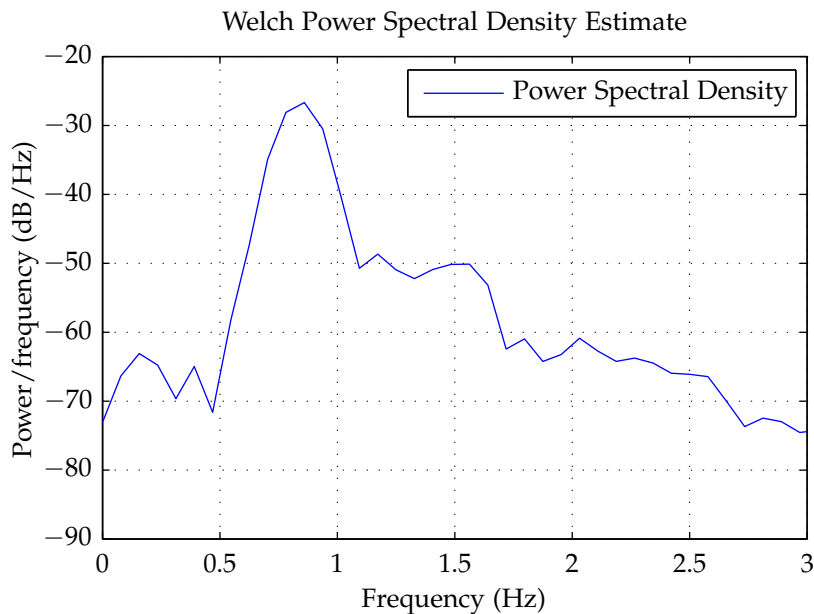


Figure 4.8. PSD of test 7 with small hanning window.

The PSD for the generated waves can be seen on figure 4.9, plotted together with the PSD from the calculated waves, using a 10 second window. It can be seen that the peak at the primary wave is slightly offset for the generated wave, compared to the expected wave. More exactly the generated wave has a frequency of 0.85 Hz. The PSD for the generated waves show a presence of energy at the frequency of the second order

component, but not as distinct as for the theoretically calculated.

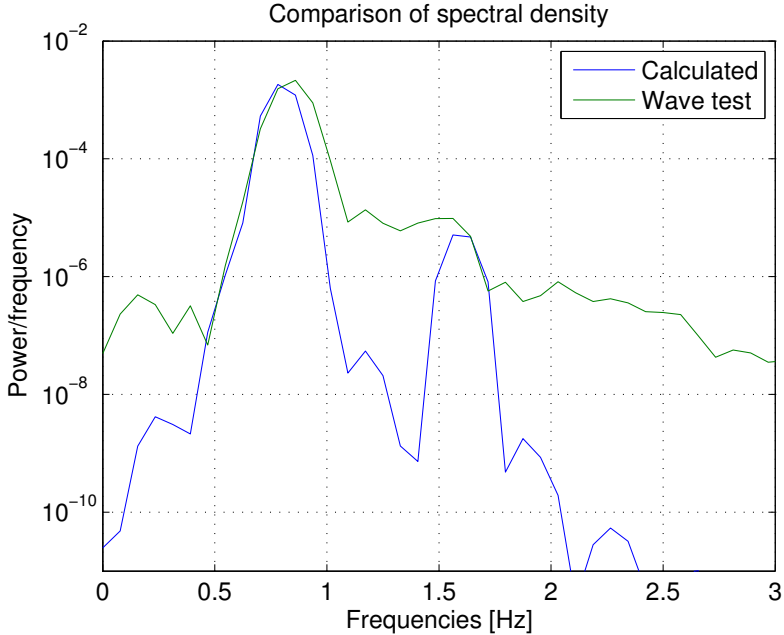


Figure 4.9. Comparison of spectral density from test 7, using 10 second window.

For the PSD using the full signal in one segment, it can again be seen in figure 4.10 that the generated primary wave has a frequency of 0.85 Hz. The second order component has however still got a frequency close to 1.6 Hz. The PSD shows a lower noise level, that contains a larger amount of energy at all frequencies, then the calculated. The power of the noise is however still several orders of magnitude lower than for the waves, so this can be neglected.

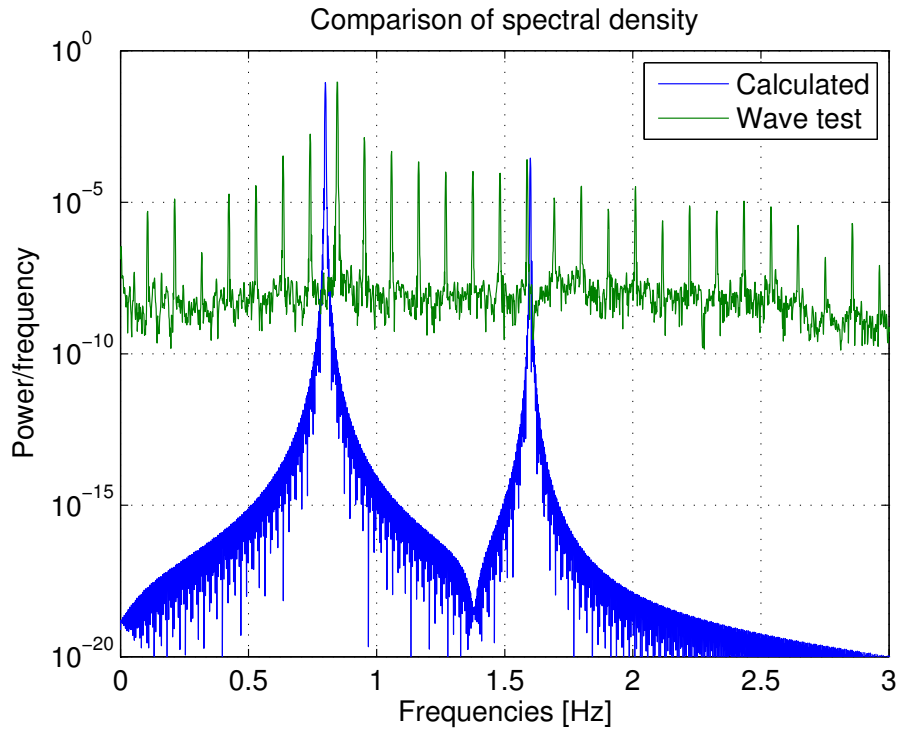


Figure 4.10. Comparison of spectral density from test 7, using 100 second window.

Test 9

The PSD of the surface elevation from test 9 is shown on figure 4.11 for a window containing the entire signal, and figure 4.12 for a window length of 10 seconds. For both the large and the small window, there is a clear peak in the energy at the frequencies of the primary waves. There are also distinct peaks of energy near the frequency difference of 0.1 Hz, corresponding to the long wave, and near the double frequencies of the primary waves. A third group of peaks can be seen from 2.5 to 3 Hz.

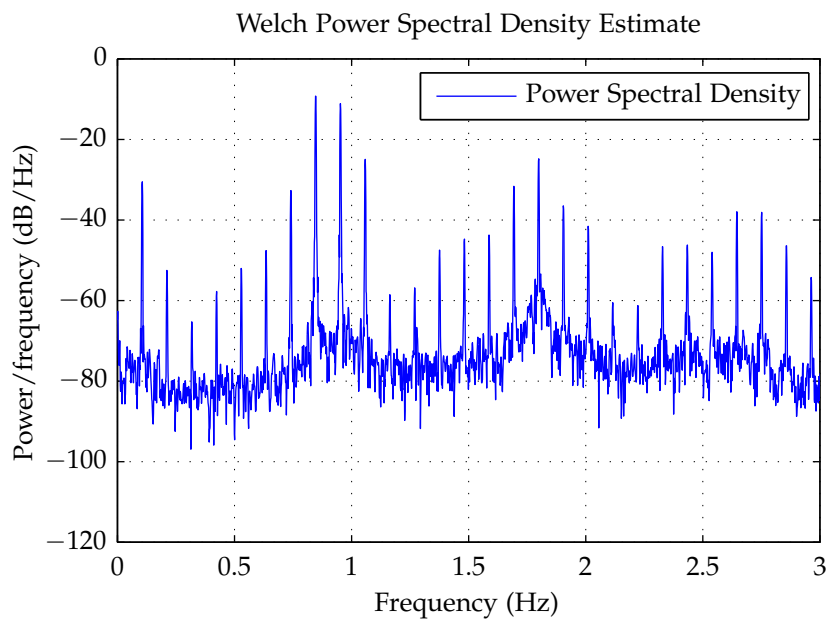


Figure 4.11. PSD of test 9 with large hanning window.

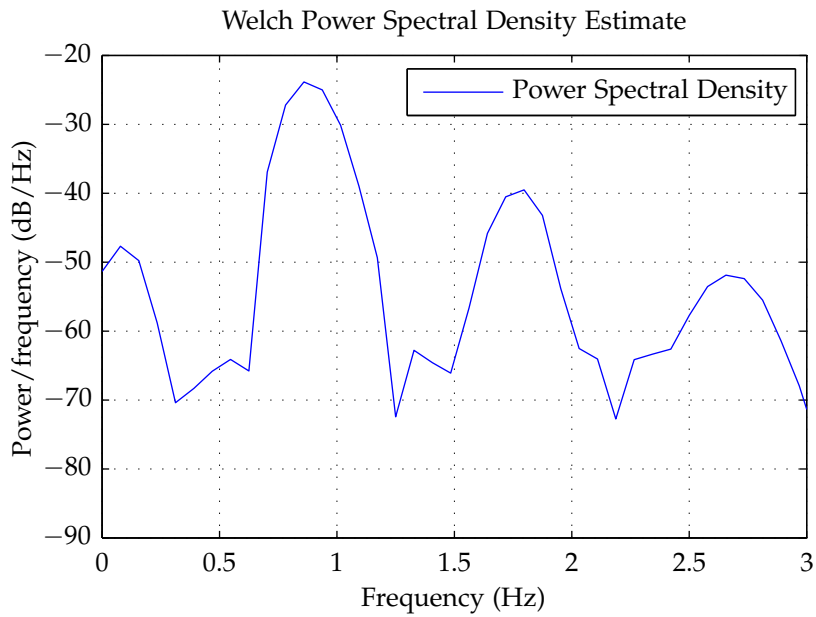


Figure 4.12. PSD of test 9 with small hanning window.

The PSD from the prediction of the surface elevation can be seen plotted together with the PSD from the testing on figure 4.13. A window of 10 seconds has been used and 50 percent overlapping. The concentrations of power at 0.1, near 0.9 and near 1.7 Hz corresponds well with the expected values. The bulge showing concentrations of power at frequencies from 2.5 to 3 Hz does however not correspond well with the input signal for generating the waves. The magnitude of the power is however quite low, which indicates that it could be caused by low amplitude reflected waves.

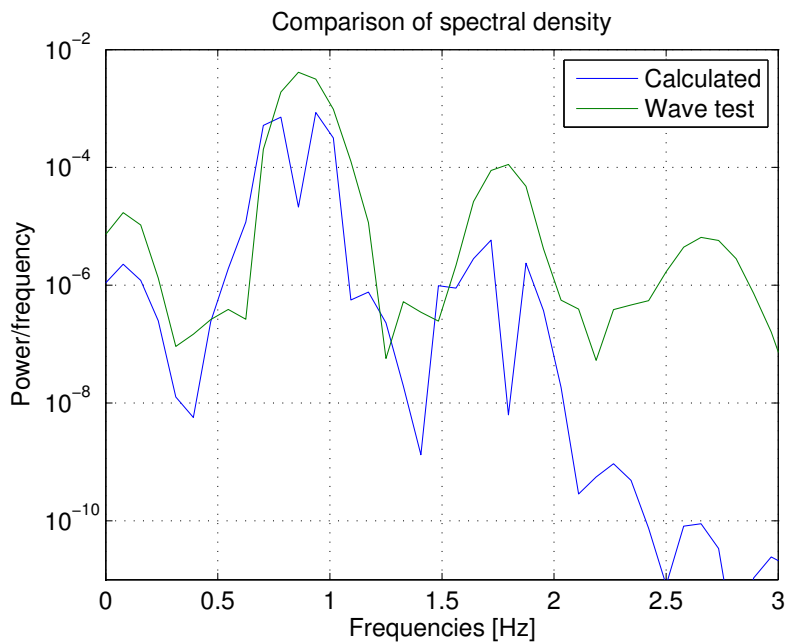


Figure 4.13. Comparison of spectral density from test 9, using 10 second window.

Again the frequencies of the two primary waves are offset from 0.8 and 0.9 Hz to 0.85 and 0.95 Hz, as a result of the offset of the waves in test 7 and 8. This can clearly be

seen on figure 4.14, showing the PSD of test 9, with a full window.

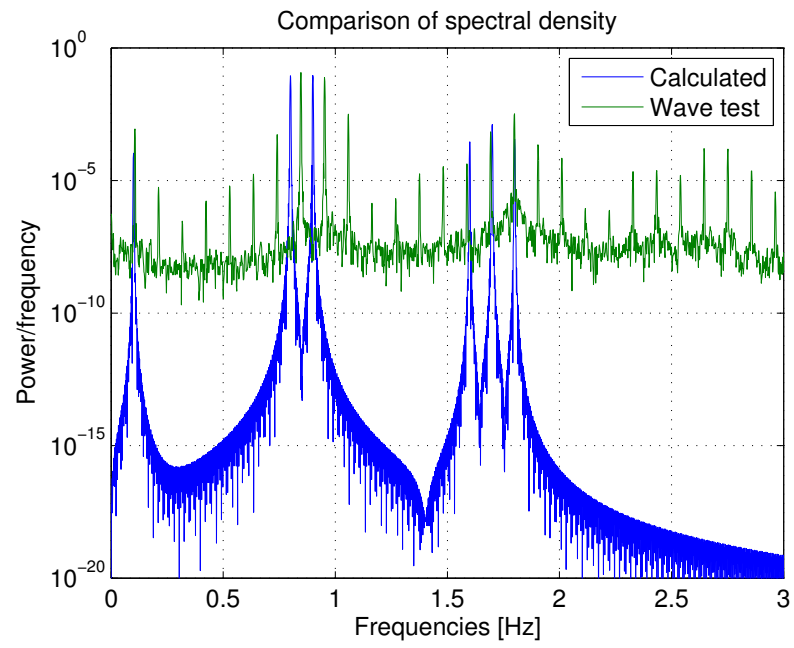


Figure 4.14. Comparison of spectral density from test 9, using 100 second window.

5 Test Setup

In this chapter the setup of the laboratory testing will be presented along with the preparations made before testing. The aim is to prepare wave flume and test model to ensure tests are performed as desired. The characteristics of the test model will be presented.

5.1 Test subject

The model used for testing is a model of a π shaped floating breakwater, consisting of a polystyren core with top and side skirts made of 5 mm aluminium plates. The dimensions of the model can be seen on figure 5.1. It can be seen that the width of the model is 980 mm, giving a 10 mm gap at each side of the model, when placed in the 1.0 meter wide flume.

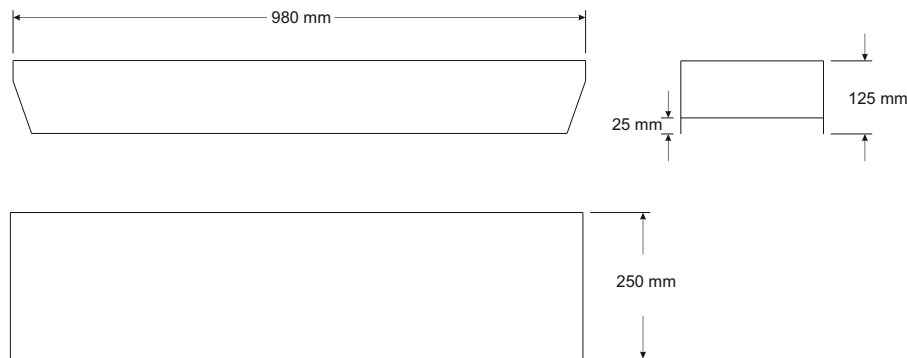


Figure 5.1. Dimensions of test model.

Table 5.1. Dimensions of model.

Length	980 [mm]
Width	250 [mm]
Height	100 [mm]
Scirt length	25 [mm]
Volume	2.3310^7 [mm ³]
Weight	14 [kg]
Freeboard	40 [mm]

The centre of gravity of the model is situated approximately 40.5 mm from the top of the model, which is just below the water line. The centre of buoyancy of the structure is the centre of gravity of the submerged part, and situated approximately 75 mm from the top of the model, as seen on figure 5.2

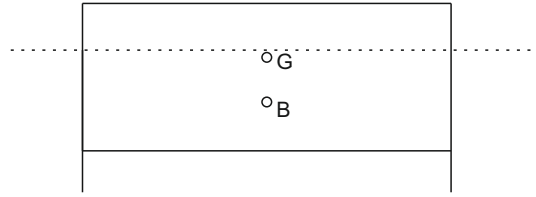


Figure 5.2. Centre of gravity G and centre of buoyancy B.

Degrees of Freedom of Model

As the model has the same width as the flume, it is restricted to movements in two directions. For a floating body, the degrees of freedom are characterised as surge for movements in the direction of the waves, heave for upward motions and pitch for rotations along the length axis, as seen on figure 5.3.

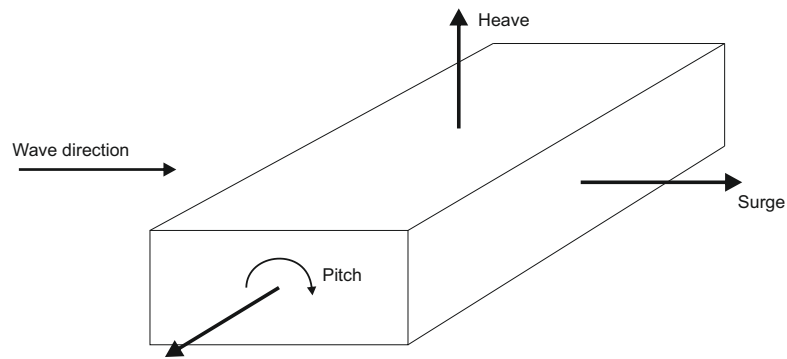


Figure 5.3. Degrees of freedom of the floating breakwater.

5.2 Mooring Systems

The model of the floating breakwater is moored using a system of four catenary lines. The catenary lines are attached at four fairlead positions, situated near the corners of the model. The catenary lines ensure the stability of the floating model, by the restoring forces generated by the weight of the chain during displacement. The chains are attached as crossing chains, which can be seen on figure 5.4.

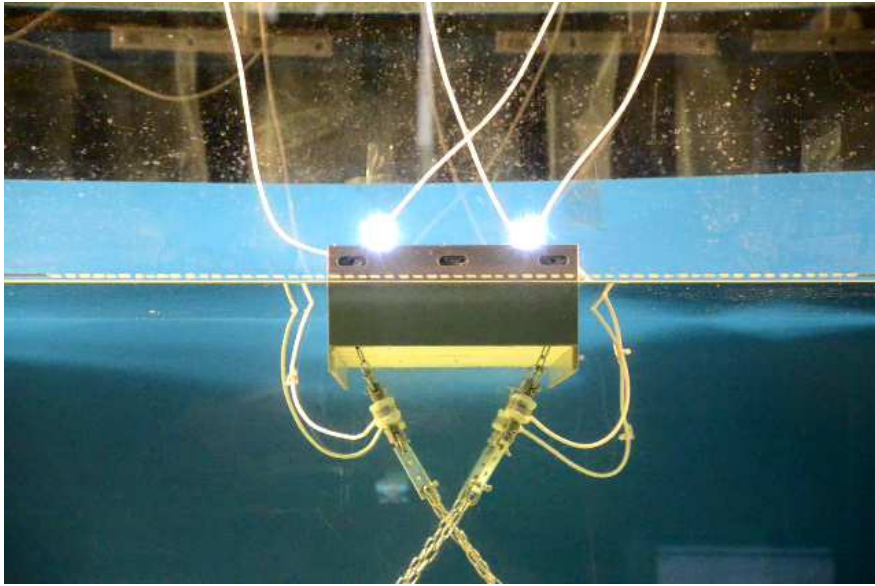


Figure 5.4. Picture of the test model with crossing chains before performing a test.

The period of the surge motion for the mooring system is measured to 10 seconds, by applying a forced displacement and releasing. The period is found by the recordings from the strain gauges in the mooring lines, as shown on figure 5.5.

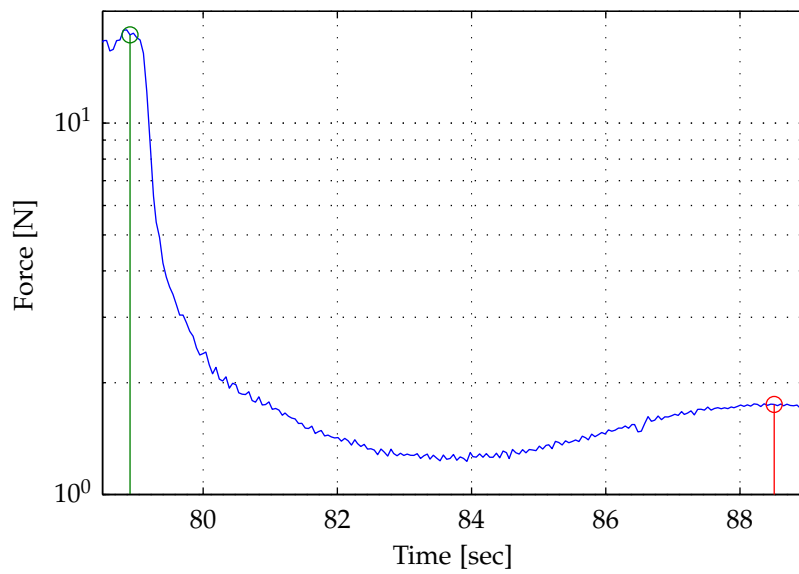


Figure 5.5. Measurement of the period of surge motion.

6 Analysis of Test Results

In this chapter the recorded movements from the object detection will be presented and analyzed in order to do a comparison with the results from the wave testing shown in 4 - *Wave Testing*. The Response Amplitude Operator or RAO, will be produced for every test, giving a transfer function between the spectrum of the waves and the spectrum of the movements. Due to this a close to linear response is expected from wave height to heave movements.

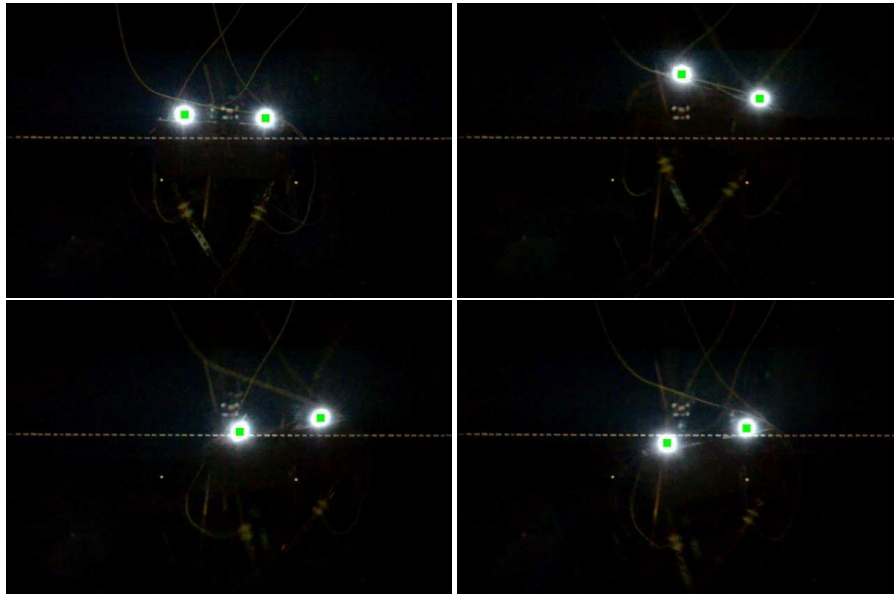


Figure 6.1. Motions of the breakwater, tracked by object detection

6.1 Movements of Breakwater

The movements of the moored floating breakwater were recorded and found as described in chapter 3 - *Motion Detection of Breakwater*. A segment of the heave movements from test 7, 8 and 9 is presented in figure 6.2. It can be seen that the heave movements resemble very well the surface elevations from the corresponding tests. This is as expected, as the a floating body would follow the surface elevations, giving a close to linear response from the waves to the heave motion for both the monochromatic and bichromatic waves.

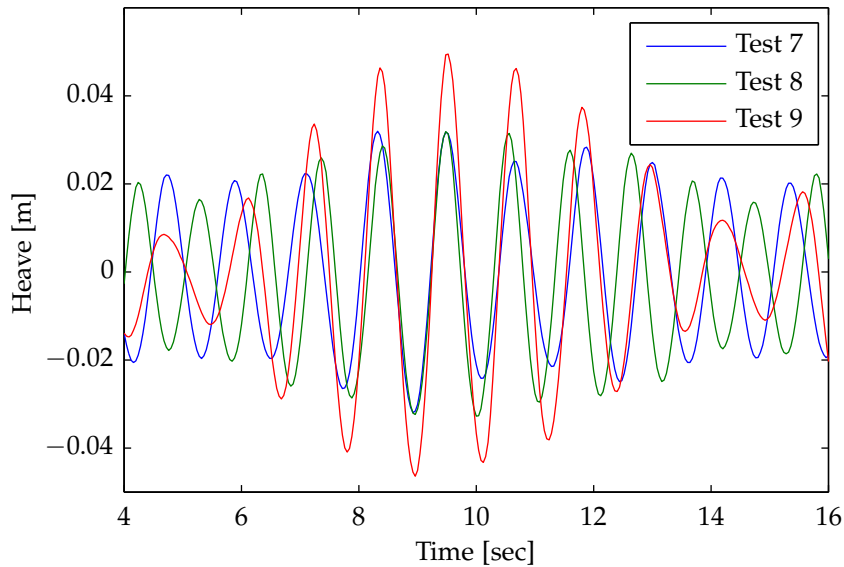


Figure 6.2. Segment of recorded heave movements for tests 7, 8 and 9.

The surge motions are contrary to the heave motions expected to have a nonlinear response, due to the effect of the nonlinear wave components. A segment of the recorded surge motions from test 7, 8 and 9 is shown in figure 6.3. It can be seen that the surge motions as expected look more nonlinear than the heave motions, and the surge for test 9 is close to four times larger than for test 7, though the wave height is only two times larger. If the monochromatic waves had been completely linear, the surge for test 7 and 8 had been expected to be closed periodic circles for every wave period. This is however not the case, both due to the nonlinearity of the waves and the imperfect generation of the waves as described in 4 - *Wave Testing*. It can be seen that be seen that the surge motions for test 8 are much larger than for test 7, even though the same wave height is used for both tests. This can be due to the waves in test 8 being more in the form of a wave group, and thus including some of the nonlinear components wanted to be examined for test 9. This will be further discussed later.

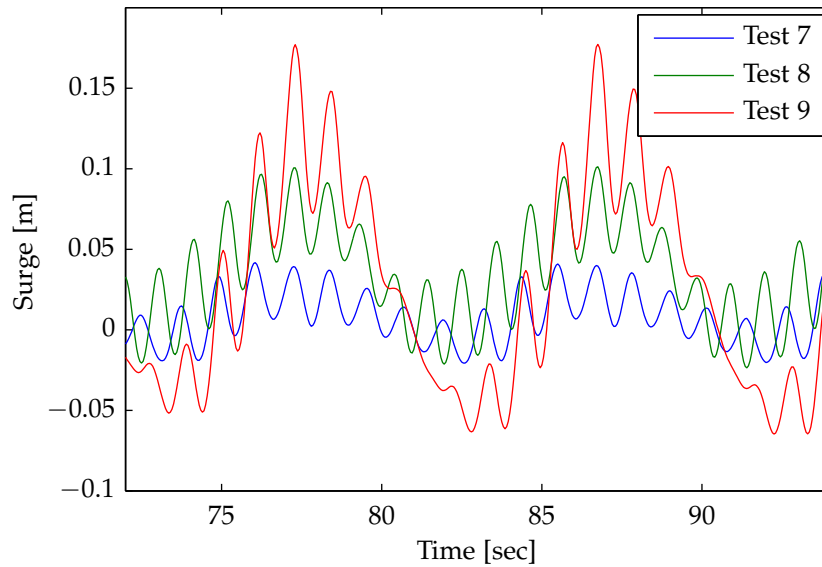


Figure 6.3. Segment of recorded surge movements for tests 7, 8 and 9.

6.1.1 Response Amplitude Operator

The nonlinear response in the motions of the breakwater can be described in form of the Response Amplitude Operator (RAO). The RAO can be from of direct comparison of wave height and displacement, but as the motions of interest occur due to nonlinear wave components, the comparison will here be made in frequency domain. This is done by calculating a transfer function between the PSD of the wave and the PSD of the motions as,

$$T_{xy}(f) = \frac{P_{yx}(f)}{P_{xx}(f)} \quad (6.1)$$

$T_{xy}(f)$	Transfer Function value from input signal xx to output yx for frequency f
$P_{yx}(f)$	PSD value of output signal for frequency f
$P_{xx}(f)$	PSD value of input signal or frequency f

Response From Surge

The response from the surge motions is found by using the MATLAB function *tfestimate*, which is using equation 6.1 to produce an estimate of the transfer between two signals. The input signal is the surface elevation of the wave testing, and the output signal is the recorded surge motion for the corresponding test. Figure 6.4 shows the PSD of the surface elevations for test 7, 8 and 9. Test 9 with the summation of the primary waves in test 7 and 9, clearly wraps the both the primary frequencies at 0.8 and 0.9 Hz, which at the wave generation came out at 0.85 and 0.95 Hz. The presence of the superharmonics is clearer for test 9, which contains three high frequency waves. The subharmonics or the long wave, should only be present for the summation of the waves in test 9, this is not the case, as some energy is present for test 7 and 8, but clearly less than for test 9.

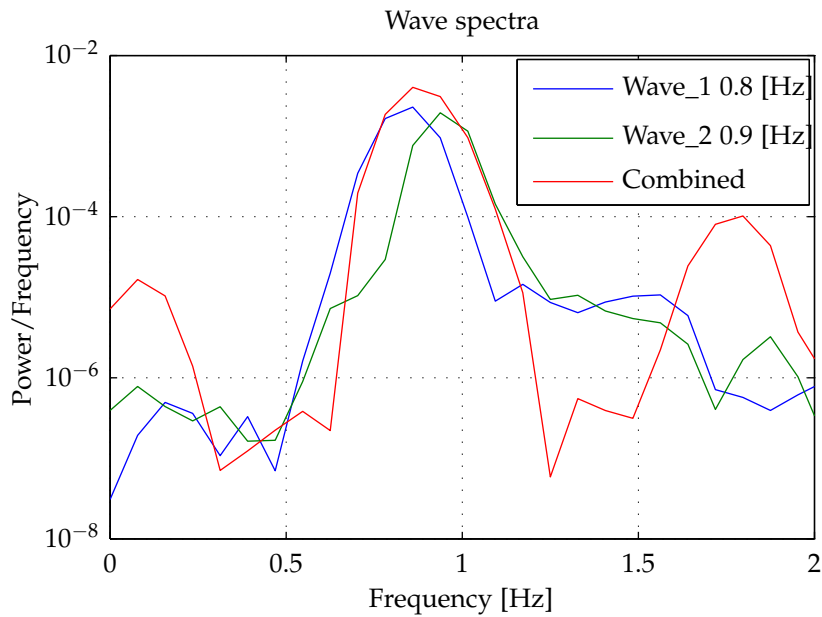


Figure 6.4. Test 7,8 and 9 wave spectrum.

The PSD of the surge motions for test 7, 8 and 9 can be seen on figure 6.5. It can be seen that the power of the movement at the low frequencies is very high for all the tests. The power at 0.1 Hz of test 8 is almost as high as for test 9 which is surprising, as the energy of the surface elevation in test 8 at 0.1 Hz was considerably lower. For test 7 the power at 0.1 Hz is lower but still at the same level as at 0.8 Hz for the primary wave.

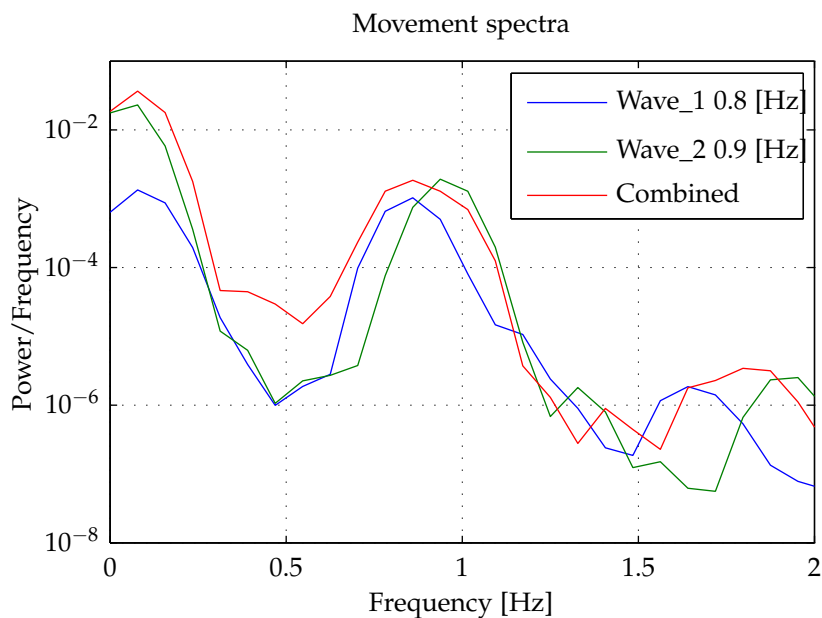


Figure 6.5. Test 7,8 and 9 movement spectrum.

The RAO of the surge movements for tests 7, 8 and 9 is shown on figure 6.6. The RAO shows that for all the tests, the response near the primary frequencies is close to one. This means that for the linear part of the wave the response is linear, in correspondence with the linear wave theory. The response of the low frequency waves show, that there is a greater response for tests 7 and 8 than for test 9. This is unexpected, as the single wave

should not contain energy at this frequency. The explanation for the higher response in the RAO is that surge motions are generally large for the single waves, while the energy of the waves is low compared to test 9. This does however not answer the question of the large motions, which seem to occur out of almost no energy in the wave. One explanation could be that the single waves, especially from test 8 with a frequency of 0.95 Hz, creates a resonance condition with the mooring system of the breakwater.

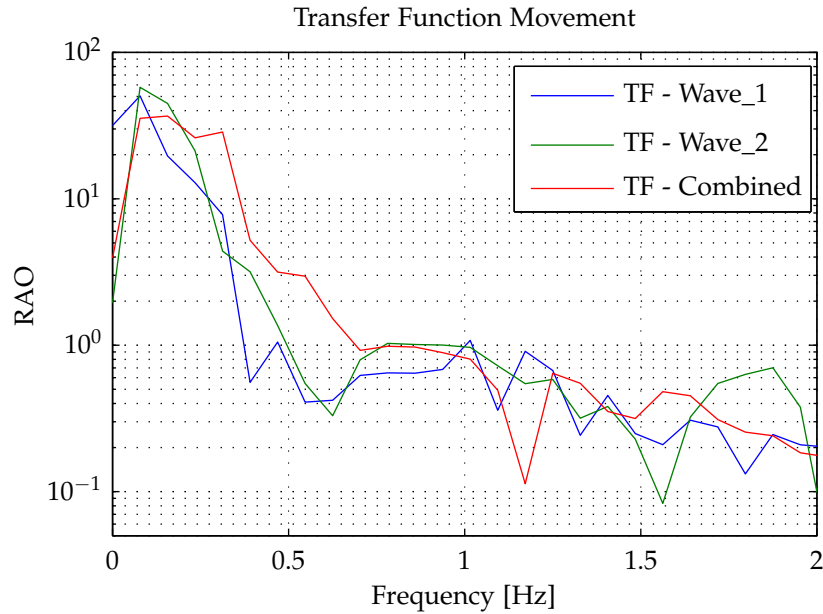


Figure 6.6. Transfer function for test 7,8 and 9.

Response from Pitch

The pitch of the model is as seen on figure 5.3, as the rotation around the length axis, perpendicular to the direction of the waves. The pitch is found from the slope between the two LEDs during testing. Due to this it is expected that steep waves will give a large contribution, while the long low frequency wave will give a lower contribution. The PSD of the pitch motions confirms this, as the power is several orders of magnitude lower for the long wave, than for the primary waves. The PSD of the pitch is shown on figure 6.7, and it can be seen that the spectrum much resembles that of the waves.

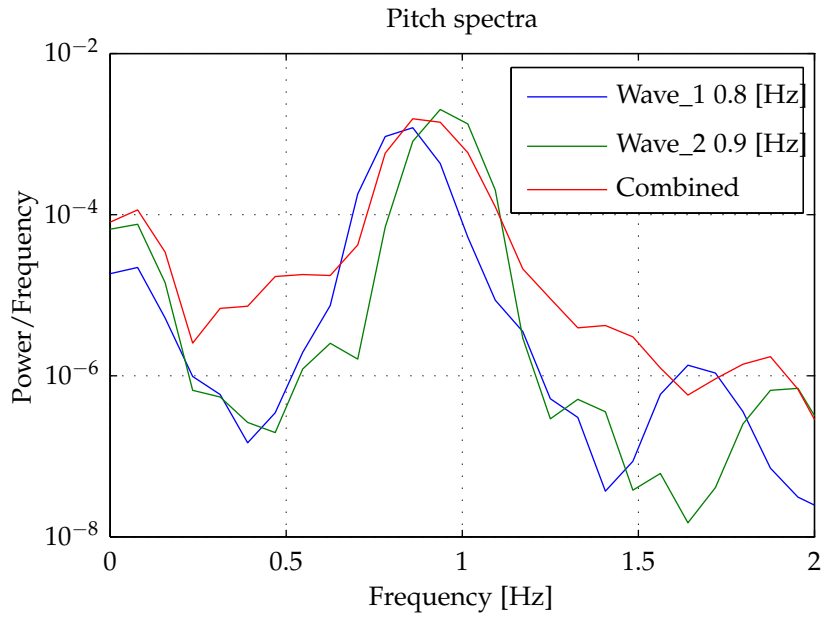


Figure 6.7. Test 7, 8 and 9 pitch spectra.

The transfer function for pitch motions shows that over all the response is close to zero, test 8 and 9 show some peaks near 0 to 0.2 Hz, as these tests contain more power for the pitch. This corresponds with the observations from the surge motions, which test 8 and 9 shows a clearer presence of nonlinearity at the lower frequencies. There are two distinct peaks at 0.4 and 0.6 Hz for test 9, these frequencies the power of both the pitch and the surface elevation is very small, meaning that small insignificant variation can give a large transfer. This large response can of course be ignored, as it does not represent any real presence of energy.

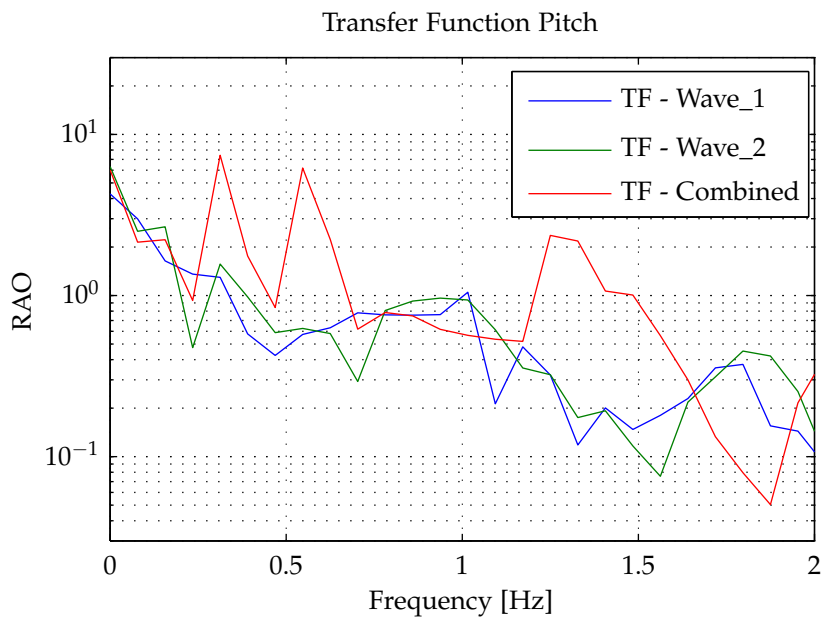


Figure 6.8. Test 7, 8 and 9 pitch TF

6.2 Forces in Mooring Lines

In this chapter the forces occurring in the mooring lines will be analysed. The forces in the mooring lines were recorded by the four installed strain gauges. The DAQ acquisition rate was 100 Hz, which was decimated to a logging rate of 20 Hz. The data was not filtered before storing. In figure 6.9 a segment of the unfiltered recorded data can be seen. It is clear that a lot of noise is present in the signal. When applying a fifth order Butterworth filter, with a lowpass frequency of 5 Hz, the same signal filters to the one seen in figure 6.9. The filtered signal does not represent the original signal well, the high frequency noise is filtered out, but the peaks in the forces are reduced as well. The high peaks in the forces occur due to snapping in the chain, which can be considered as an instantaneous load, applied at a very high frequency.

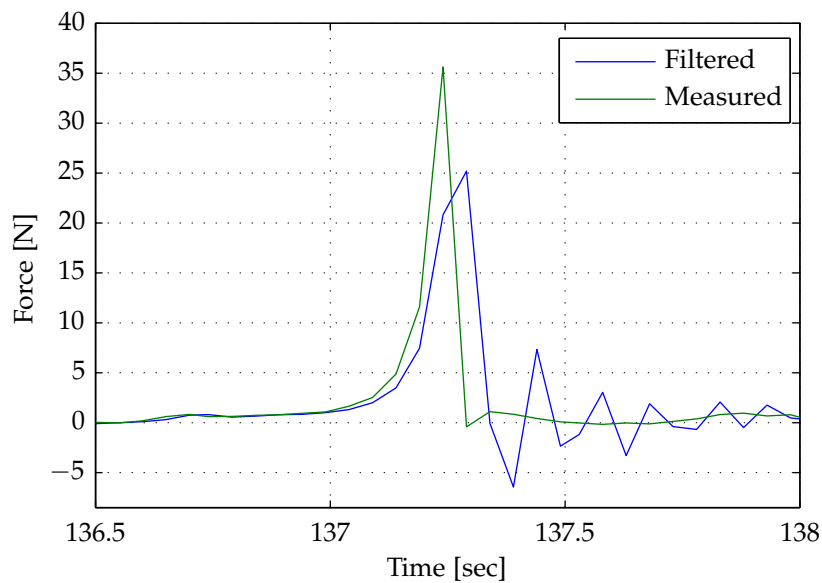


Figure 6.9. Section of recorded and filtered forces from test 9.

For the tests where snapping does not occur, applying a low pass Butterworth filter, with a cut off frequency of 5 Hz gives as good fit.

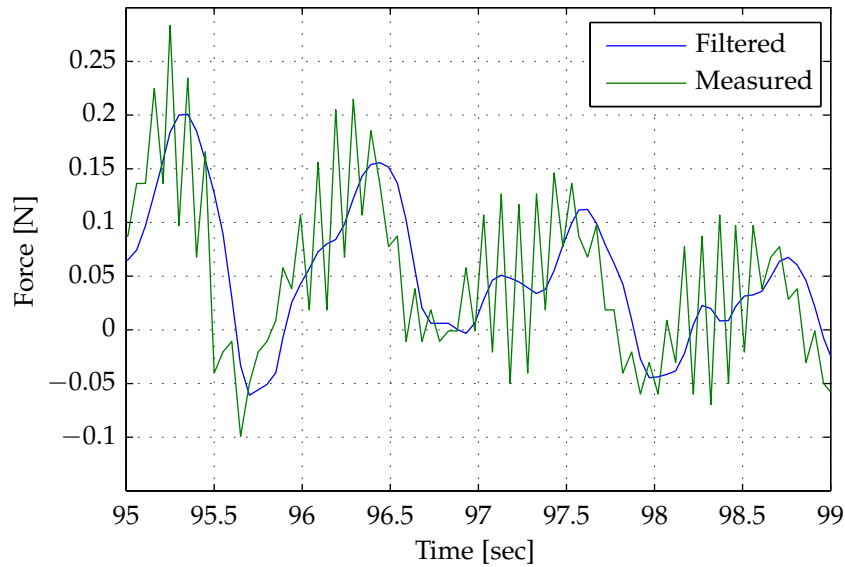


Figure 6.10. Section of recorded and filtered forces from test 7.

Although the test without occurrence of snapping gives good results when filtering, the unfiltered data will be used for the further analysis, in order to have completely comparative input and results.

Transfer function - Wave-force

From the PSD of the forces from tests 7, 8 and 9 it is clear that for all tests the largest concentration of power is near 0.1 Hz. The areas near the primary waves and the high frequency waves are also clearly distinguishable by concentrations of power. For test 9 the level of power for all frequencies from 0 to 3 Hz, is significantly higher than for test 7 and 8. This can be caused by a combination of the resonance from the long waves, and the snapping forces occurring in the mooring lines. The snapping causes a lot of vibrations in the chain, possibly varying across a wide range of frequencies.

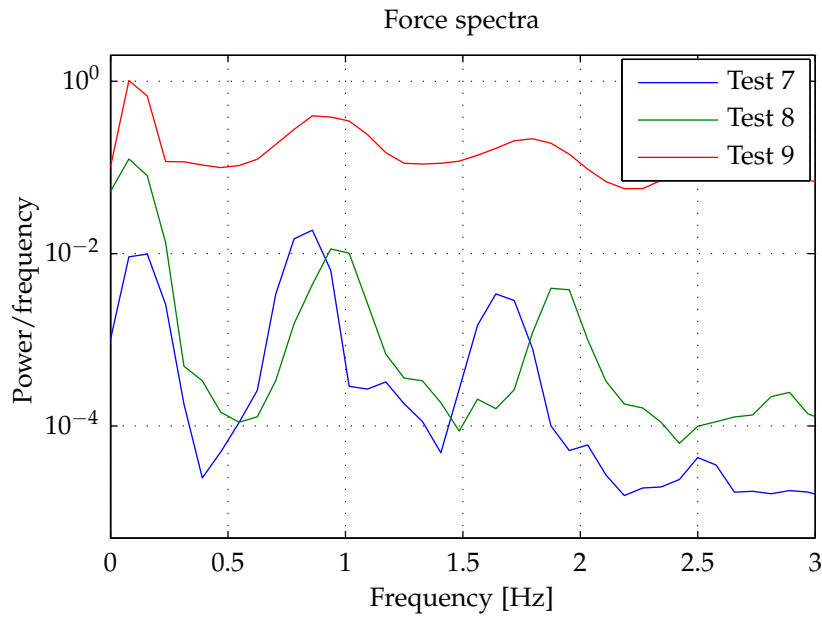


Figure 6.11. PSD of chain forces from tests 7, 8 and 9.

When producing the transfer function between the waves and the forces in the mooring lines, it can be seen that the wave test with the bi-chromatic waves holds the largest amount of power from the forces compared to the power from surface elevations. The distribution of the power over spectrum is however not so clear. There is a large response at 0.1-0.6 and again from 1.2-1.6. This can perhaps be explained by the lack of energy in those regions in the wave spectrum, while as explained the PSD of the forces from test 9 contains a large amount of power at all frequencies. This gives an unexpected transfer from test 9, while the transfer for tests 7 and 8 looks as expected, with a large response at the lower frequencies, and a response close to one near the primary frequencies.

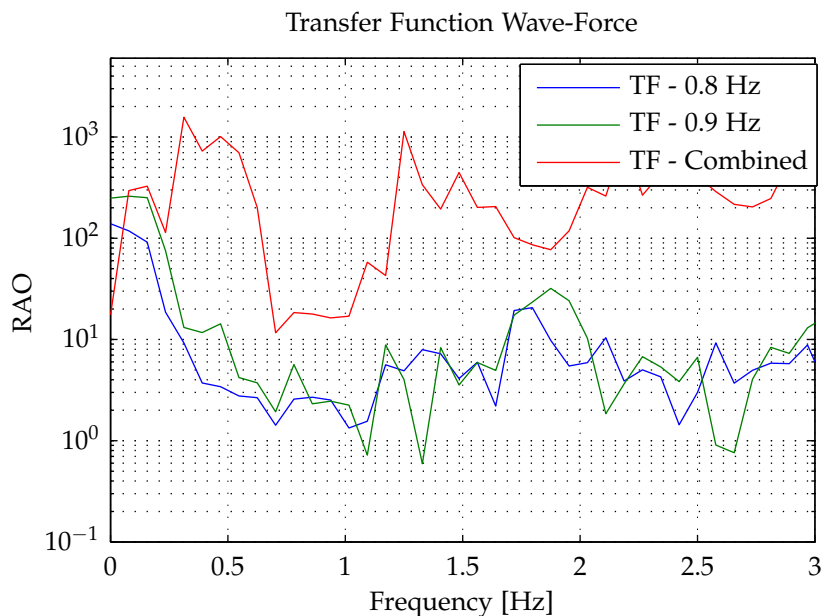


Figure 6.12. Transfer function from wave spectrum to force spectrum, tests 7, 8 and 9.

As the results for the RAO of the forces in the mooring lines did not give good results

for test 9, due to snapping in the chains, the results from tests 4, 5 and 6 are treated. The PSD of the waves can be seen on figure 6.13 and the PSD of the forces can be seen on figure 6.14. The power levels of the forces from the bichromatic waves in test 6 are again larger than for the monochromatic waves, but not as clear as for test 9.

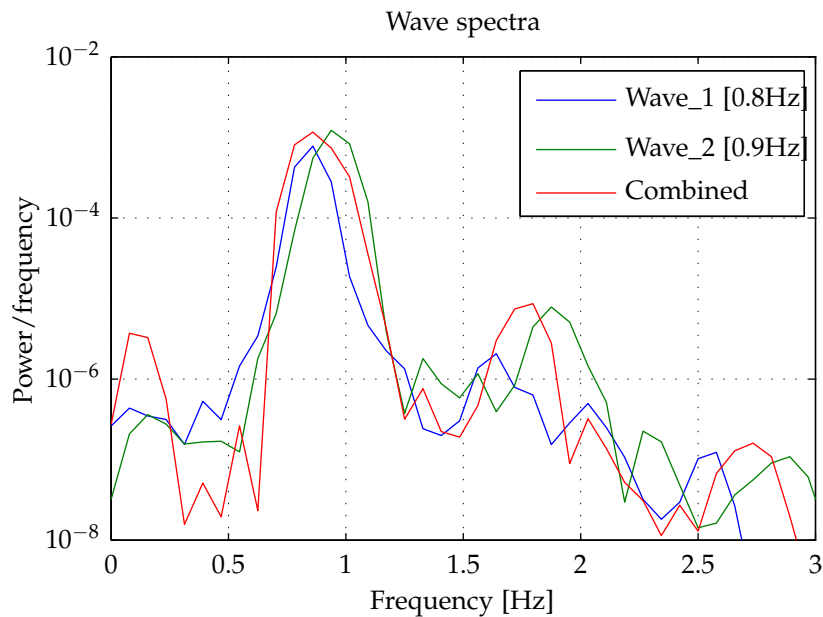


Figure 6.13. PSD of the surface elevations from test 4, 5 and 6.

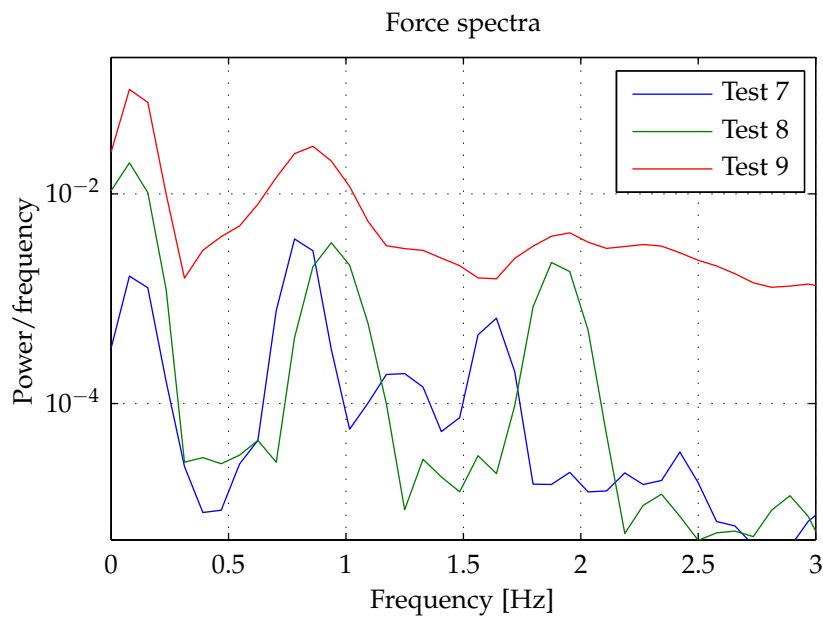


Figure 6.14. PSD of the mooring forces in test 4, 5 and 6.

The RAO of the force for tests 4, 5 and 6 is plotted on figure 6.15. The response can be seen to be more in correspondence with the expected, as all tests show a large response at the low frequencies, decreasing towards the primary frequencies. From this it is clear that the snapping in the chains creates some disturbances, hiding the actual response of the structure.

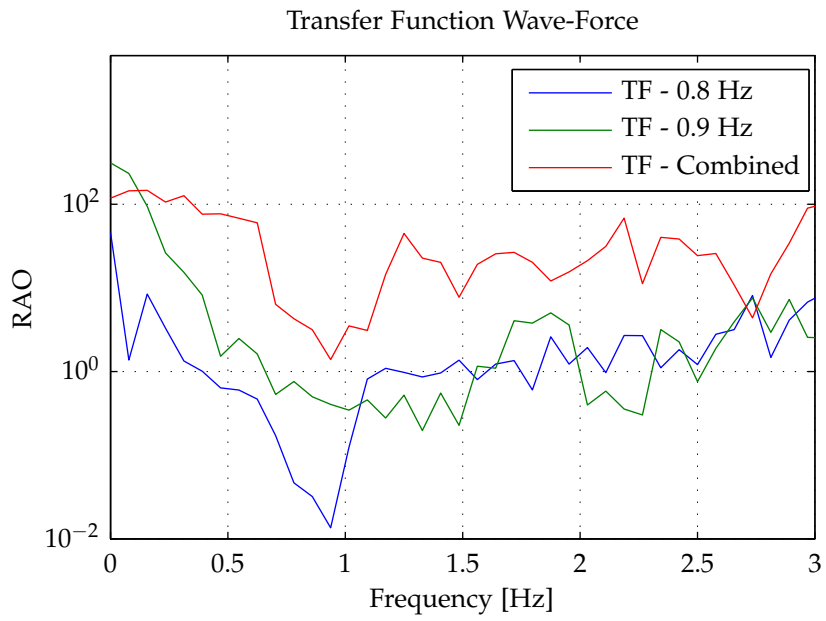


Figure 6.15. Transfer function from wave spectrum to force spectrum, tests 4, 5 and 6

7 Discussion

In this chapter the methods used in the project will be discussed along with the obtained results. The final results will be summarized and concluded upon, leading up to the final conclusions.

The aim of the laboratory testing was to produce two series of monochromatic waves, and a bichromatic series containing the summation of the two first wave series. By doing so, the response of the moored floating construction could be observed for the single waves and for the summation, where the presence of high and low frequency second order components were expected. The generation of bichromatic waves were however not completely possible with the available software, as the generation had to be done as a custom spectrum using white noise generation. The output of spectrum containing a single monochromatic wave can be seen in figure 7.1 along with the predicted output for a single wave, using the second order PTF that was used as the control signal. It can be seen that due to the use of repetition of 10 second white noise distributed signals, the generated waves assume a grouping behavior, though only containing one primary frequency with varying amplitude. The output frequency has also been altered during the generation to approximately 0.85 Hz instead of 0.8 Hz. This could be due to wave generator being of older date, and not reproducing the correct signal.

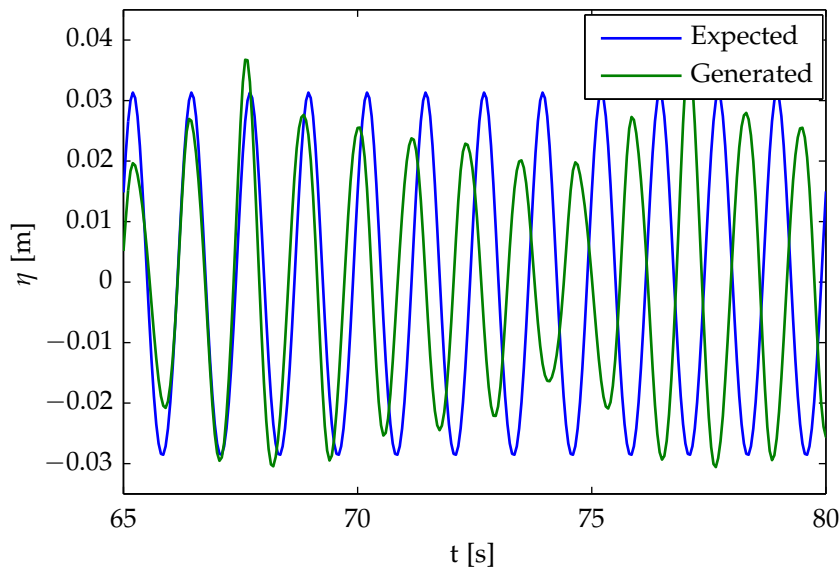


Figure 7.1. Comparison of the expected and the generated waves.

The monochromatic waves did not reproduce well, and the generated signal shown on figure 7.1 initially seems to vary too much from the desired to be of use for the testing. The generated signal of the bichromatic waves does however give decent results, and the comparison of desired and generated waves on figure 7.2 shows good resemblance. Again it is observed that the generated frequency of the waves does not correspond with the expected, as a result of the frequency error from the bichromatic waves.

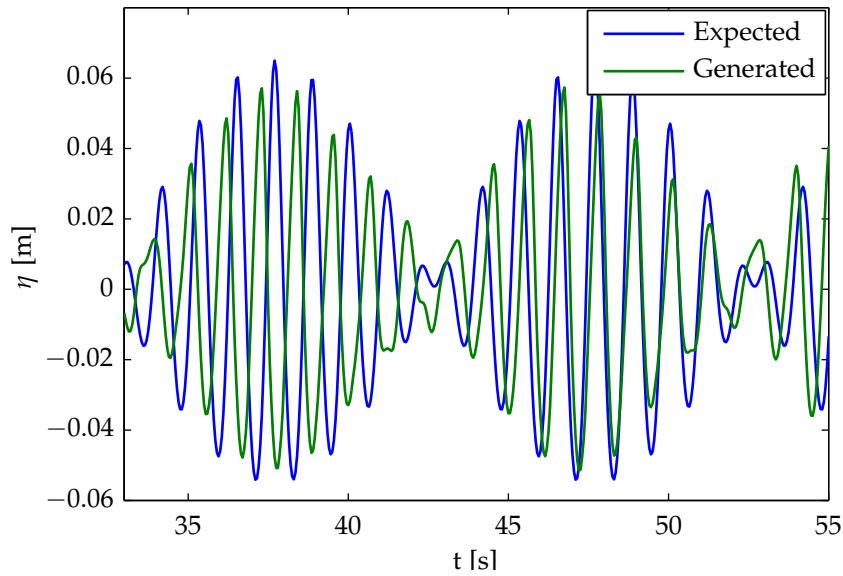


Figure 7.2. Comparison of the expected and the generated waves for bichromatic waves.

As the waves are generated using white noise distribution, and the signal is repeated every 10 seconds, a significant error is induced. This means that an analysis using the described waves cannot possibly give the desired results, and the method is very questionable. Under the given circumstances, there were however no alternative methods, which is why the tests were carried on. This means that during the analysis of the testing, the error due to the wave generation needs to be considered.

The transfer functions from the surface elevations to the motions and forces, where very spiky and not very clear. For most part this is due to the relation between the parts of the spectra containing little or close to no energy. A method to avoid this, could be to remove the parts of PSD that does not contain much energy, in order not to divide by close to zero, and get a huge response at frequencies with no power. A simplified version of this has been used to produce the plots in figure 7.3 and figure 7.4, showing the response at 0.1, 0.8 and 0.9 Hz for the surge motions and forces. The response of the surge motions on figure 7.3, are plotted so the response from the primary monochromatic waves are at 0.8 and 0.9 Hz, while the response from the long waves in the bichromatic tests are plotted at 0.1 Hz.

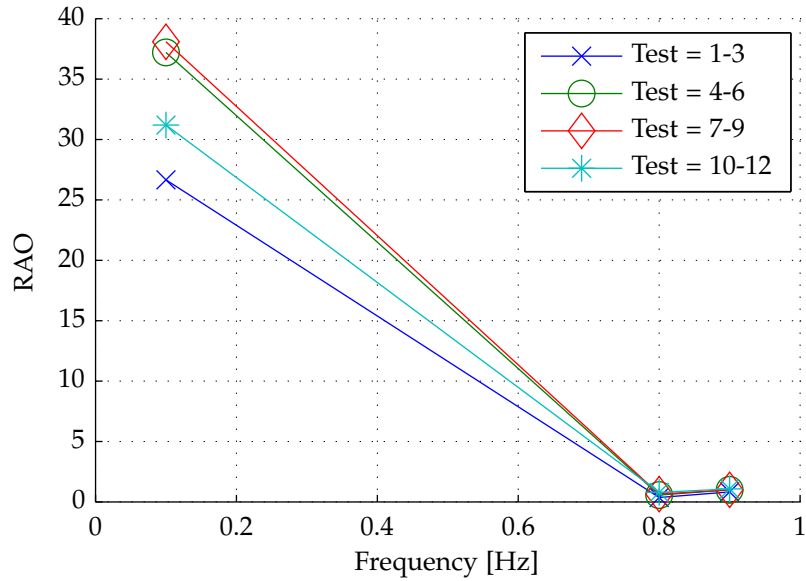


Figure 7.3. RAO's for all tests.

The response of the forces is plotted as for the surge motions and, it can again be seen that the low frequency response is dominating and increasing along with the wave height of the test. The snapping occurring in the chains at the larger wave heights, gives an unrealistically large response and covers the phenomenon that is investigated. The mooring system was designed to fit the long period of the generated waves giving a period of the mooring of 10 seconds, the design was however not ideal.

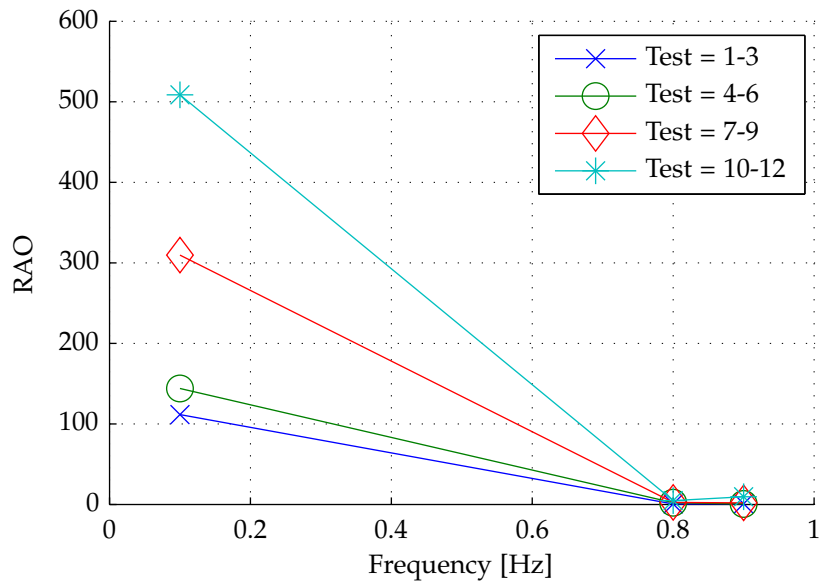


Figure 7.4. RAO's of forces for all tests.

8 Conclusion

This thesis has studied the effects of second order waves on a moored floating breakwater. The investigated waves have been series of monochromatic waves and the corresponding summation into series of bichromatic waves. The simplified theoretical surface elevations have been calculated using a second order transfer function. The same transfer function is used to generate the second order control signal for movements of the wave paddle. In this way the theoretical output of the wave generation has been obtained.

A non disturbing system to detect the motions of the floating breakwater has been developed. The tests were recorded using a video camera, storing the movements as a movie file. The system tracks the movements of the breakwater by a simple form of optical object detection. The system gives good results, and the output is considered to be precise enough for the analysis.

The wave generation did not yield good results, as it was not possible to generate the desired waves. The final waves used for testing were a compromise between the need of waves in order to finish the thesis, and inducing a significant error into the results, by using incorrect waves. Though not being generated correctly, the Power Spectral Density of the waves shows correspondence with the theoretical. The presence of the low frequency long wave is clearly observed for the bichromatic waves. The model of the floating breakwater was measured to have a surge period of 10 seconds, and the frequency difference of the monochromatic waves was set to 0.1 Hz, in order for resonance to occur with the long waves from the wave grouping.

The analysis of the tests with the floating breakwater includes the forces measured by the strain gauges in the mooring lines, and the motions of the breakwater, obtained by the motion detection system. The data was analysed in order to find the ROA of the breakwater, when subjected to nonlinear waves. The ROA of the surge motions of the breakwater, during bichromatic wave testing, show a very large response near the frequency of the long wave. The response for the bichromatic waves is even larger, but it should be taken into account that the power at the low frequencies for the monochromatic waves is several orders of magnitude lower than for the bichromatic tests. The errors in the wave generation also have an effect on this, as the movements spectra show very large response at the low frequencies for the monochromatic tests. The response of the forces was shown not to be completely reliable, as the design of the mooring system allowed snapping to occur for the larger wave heights. For the lower wave height, where snapping does not occur, the results show a nonlinear response as well.

The final remarks regarding the results obtained in the project, are that it did not succeed producing the desired waves, thus not getting the expected result out of the wave testing. However, the obtained result does show the nonlinear response of the floating breakwater, and clearly documents that the occurrence of grouped waves is critical for the design of moored constructions.

References

- Thomas Lykke Andersen and Peter Frigaard, 2012.** Technical documentation for AwaSys 6. Downloadet: 04-03-2013.
- H. Bredmose, Y. Agnon, P.A. Madsen, and H.A. Schaffer, 2005.** Wave transformation models with exact second-order transfer. *European Journal of Mechanics B/Fluids*, Volume 24, pp. 659–682.
- Nuno Fonseca, Joao Pessoa, Spyros Mavrakos, and Marc Le Boulluec, 2011.** Experimental and numerical investigation of the slowly varying wave exciting drift forces on a restrained body in bi-chromatic waves. *Ocean Engineering*, Volume 38, pp. 2000–2014.
- N. E. Ottesen Hansen, 1978.** Long period waves in natural wave trains. Prog. Rep. 46, Inst. Hydrodyn. and Hydraulic Engng., Tech. Univ, Denmark, pages pp. 13–24.
- N.E. Hansen, Stig Sand, H. Lundgren, Torben Sorensen, and H. Gravesen, 1980.** Correct Reproduction Of Group-Induced Long Waves. *Coastal Engineering Proceedings*, 1(17).
- M.S Longuet-Higgins and R.W. Stewart, 1964.** Radiation stresses in water waves; a physical discussion with applications. *Deep-Sea Research*, Volume 11, pp. 529–562.
- Paolo Pezzutto, 2013.** On Floating Breakwaters Efficiency.
- Stig E. Sand, 1982a.** Long Wave Problems in Laboratory Models. *Journal of Waterway, Port, Coastal and Ocean Division*, Volume 108, pp. 492–503.
- Stig E. Sand, 1982b.** Wave Grouping Described By Bounded Long Waves. *Ocean Engineering*, Volume 9, pp. 567–580.
- Stig E. Sand and E. P. D. Mansard, 1986.** Reproduction Of Higher Harmonics In Irregular Waves. *Ocean Engineering*, Volume 13, pp. 57–83.
- MARINTEK SINTEF.** URL: <http://www.sintef.no/home/MARINTEK/>.
- Ib A. Svendsen, 2006.** Introduction to Nearshore Hydrodynamics. 981-256-142-0. World Scientific Publishing Co. Pte. Ltd.

Part II

Appendix Report

A Object Detection

There are several different methods for identifying an object and tracking it, such as predefining certain shapes i.e. circles, lines and corners, that will be recognized on the video. An object can tracked by movement from one frame to another. A very simple and basic way to track, is to define an object by the color composition. This method has been chosen to be used in this project.

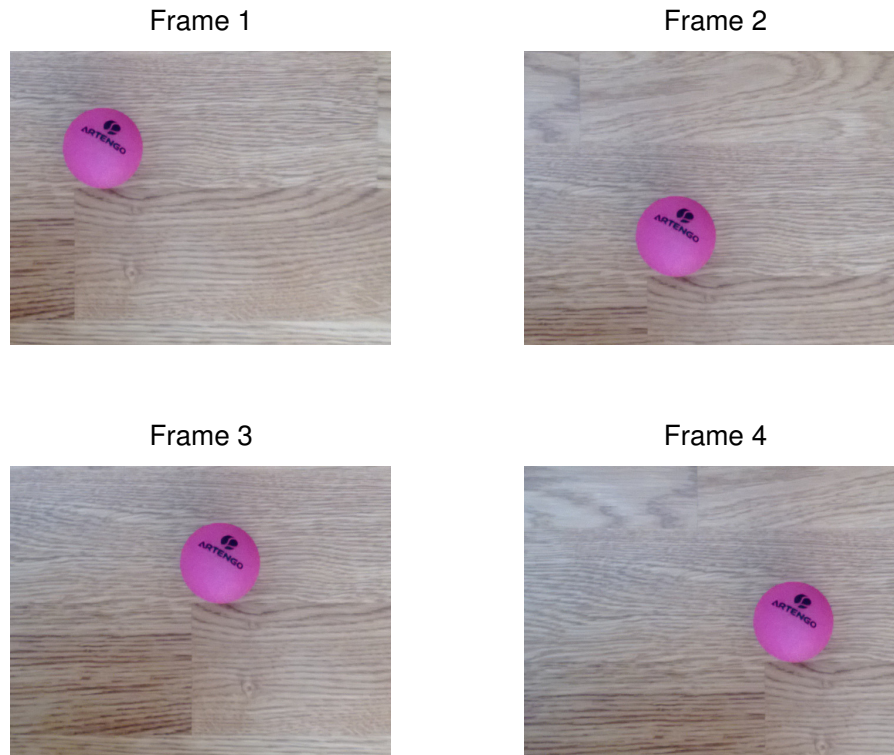


Figure A.1. Frames 1 to 4 from example of trackin a moving red ball.

The frames in figure A.1 are converted by removing all pixels outside the color composition of the ball. The *bwlabel* command of MATLAB is used, to transform the matrix in RGB color, into an emty matrix with the same size as the frame, containing ones in the entrances corresponding to the pixels of the desired color. The *regionprops* command is then used with the matrix as input. This outputs a number of objects and their properties. The objects are defined by pixels being connected in a group. The properties of the objects are the area, defined by the number of pixels connected and the centroid of each object. On figure A.2 the grouping of the frames can be seen.

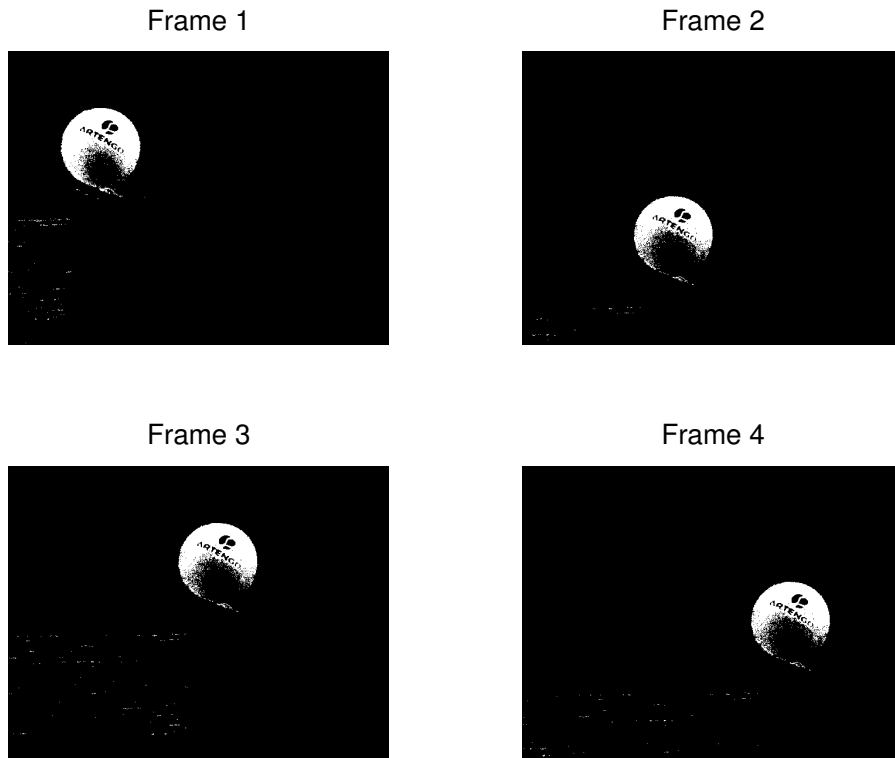


Figure A.2. Frames 1 to 4 converted to objects.

The plots show a number of scattered small objects, with the size of only a few pixels. The objects occur due to small reflections on the surface, creating color compositions equal to that of the ball, and thus creating an alias in the detection. This is among the complications and limitations of this simple method to object detection. On figure A.3 the initial frames can be seen, with a white marker plotted to illustrate the found centroid of the object. It can be seen that the centroid is slightly offset in every frame, corresponding to the missing part of the ball on figure A.2. This is due to shadowing, changing the color of the ball. This could be avoided by accepting a larger spreading in the color of an object, but this would at the same time significantly increase the aliasing. The movements of the ball, given in pixel coordinates of the frame, can be seen on figure A.4.

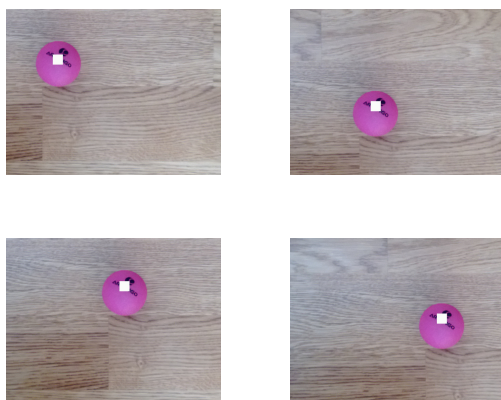


Figure A.3. Centroid of objects marked with white dot.

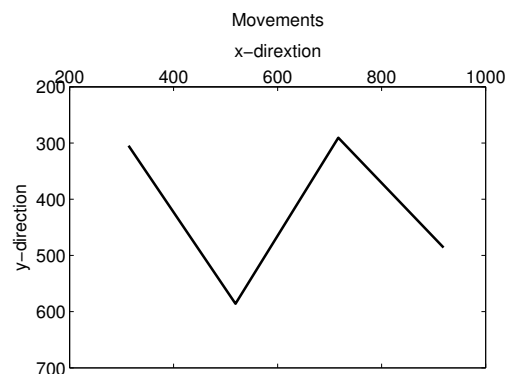


Figure A.4. Movements of the ball in pixel coordinates.

B Wave testing

This appendix contains the plots of the surface elevations for tests 1-6 and 10-12.

B.1 Waves

B.1.1 Test 1,2 and 3

Monochromatic wave one and two.

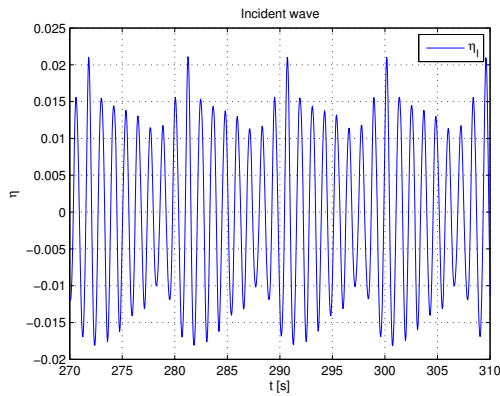


Figure B.1. Test 1 generated waves.

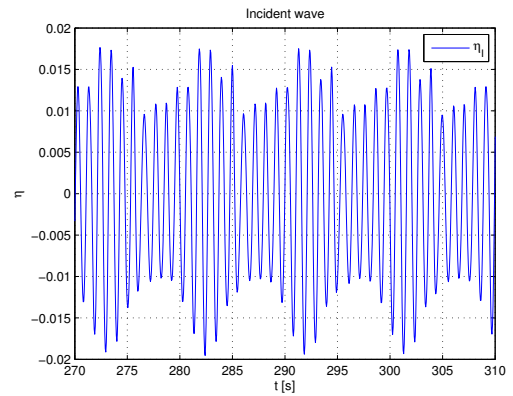


Figure B.2. Test 2 generated waves.

Bichromatic wave.

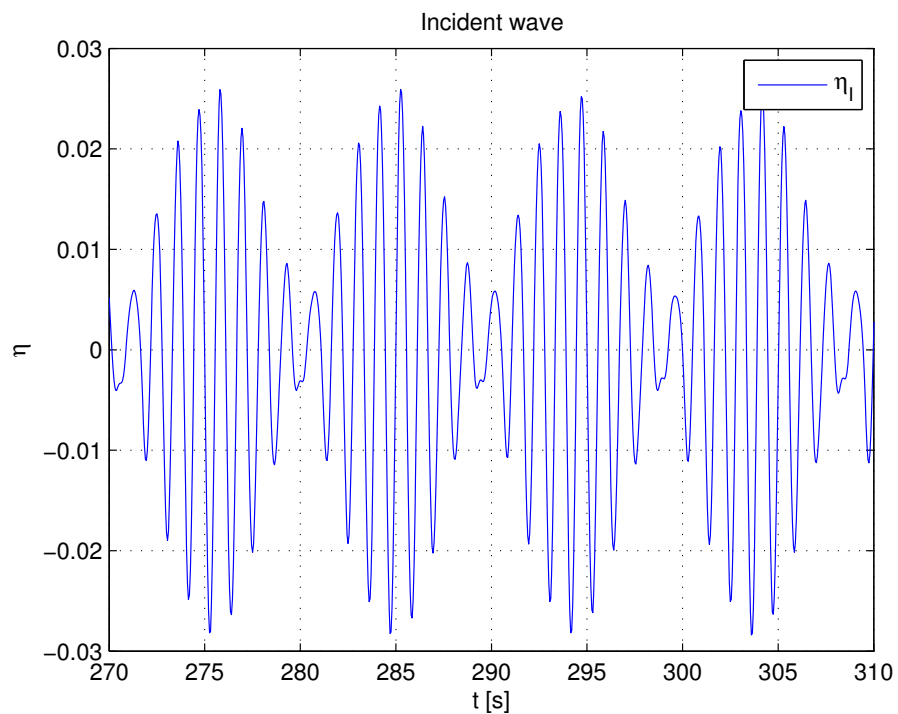


Figure B.3. Summation of waves.

B.1.2 Test 4,5 and 6

Monochromatic wave one and two.

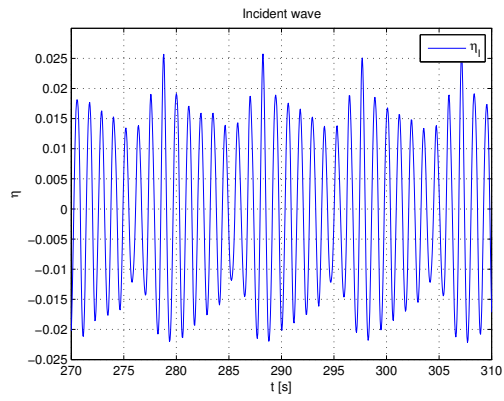


Figure B.4. Test generated waves.

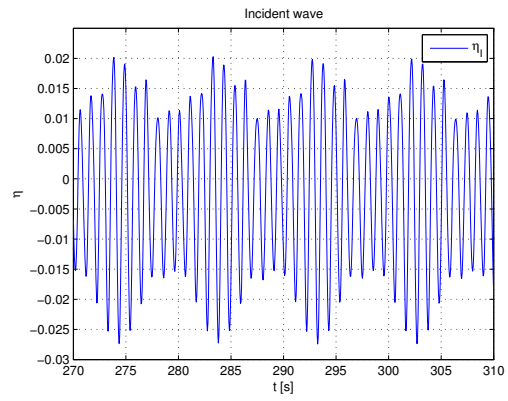


Figure B.5. Test 5 generated waves.

Bichromatic wave.

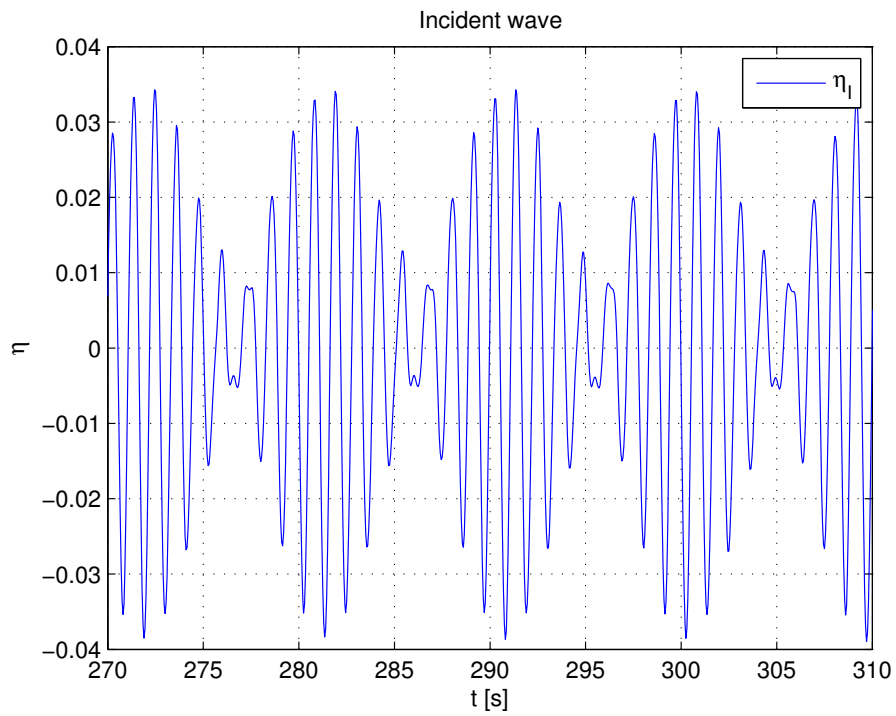


Figure B.6. Summation of waves.

B.1.3 Test 10,11 and 12

Monochromatic wave one and two.

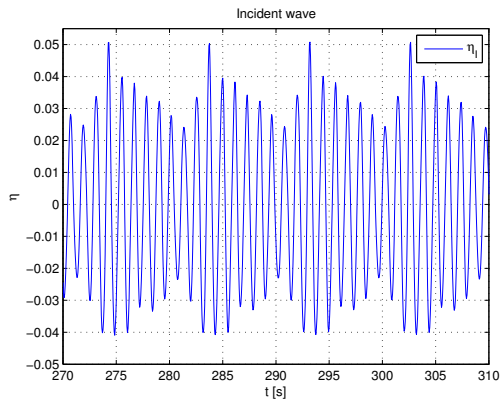


Figure B.7. Test 10 generated waves.

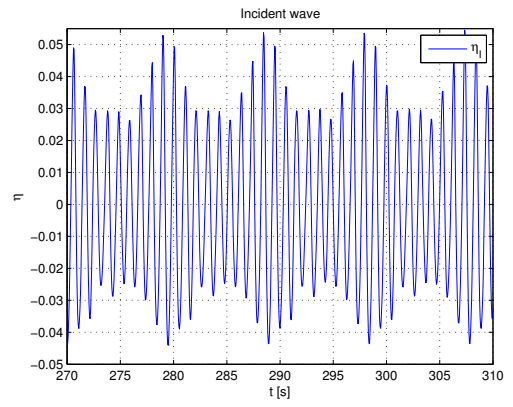


Figure B.8. Test 11 generated waves.

Bichromatic wave.

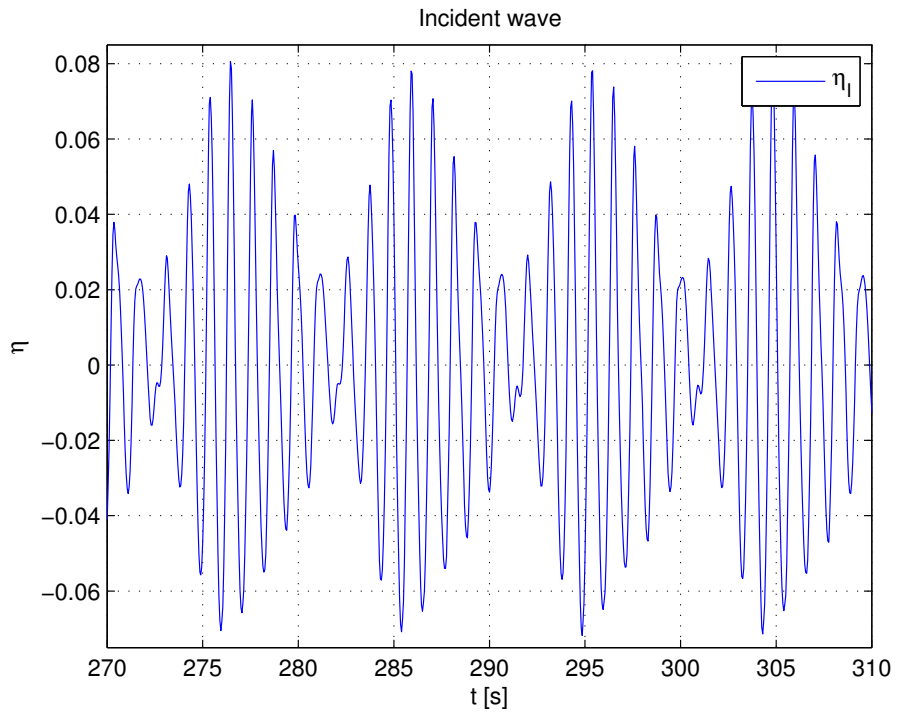


Figure B.9. Summation of waves.

C Analysis of aquisition rate

In this chapter a short analysis will be performed of the effect of acquisition rate on the logging of the forces in mooring lines.

C.1 Installing strain gauges

In order to log the data at a high enough frequency, a data logging function was constructed in the visual programming tool LABVIEW. The strain gauge is connected via a 10 pin plug, to a NI 9237 DAQ. The DAQ feeds the signal to the strain gauge, and sends the returning signal to the LABVIEW DAQ ASSISTANT. The DAQ can only log by frequencies defined by,

$$f = \frac{50.000[\text{Hz}]}{n} \quad (\text{C.1})$$

Where n is a divisor from 1-31. This gives 1612.9 Hz as the lowest possible sampling frequency, when only one channel is connected to the DAQ. When logging at 1600 Hz, a huge amount of data has to be stored, and the possessing time of the data will be very long. The solution to the problem would be to sample the data at a high frequency, and then reduce the data in bundles, so the final stored data points will be equivalent to the desired sample rate. As the desired sampling rate is 200 Hz, the first approach was to sample at 5000 Hz and thus obtain 50 data points, every 0.01 second, which was to be stored as one point. A very simple way to do this would be to use the mean value of the 50 samples, and log that as the one point. This method would not give a very smooth transition to the next point, and could create a numeric error. Instead it a low pass filter is used that imports data at 50.000 Hz, and thus have 500 points, every 0.01 second. The filter removes all frequencies above a threshold of 50 Hz, and sends 500 filtered points on to a decimator, that reduces the 500 points to two points, and thus saving the data at ≈ 200 Hz.

DAQ logging

The strain gauges used for testing were installed on metal rods, and coated in impermeable material in order to use them for measurements in the flume.

The following results are from a test run with a setup of strain gauges, logging at different frequencies. Below is shown a comparison of two gauges, one logging at 400 Hz and the other at 20 Hz.

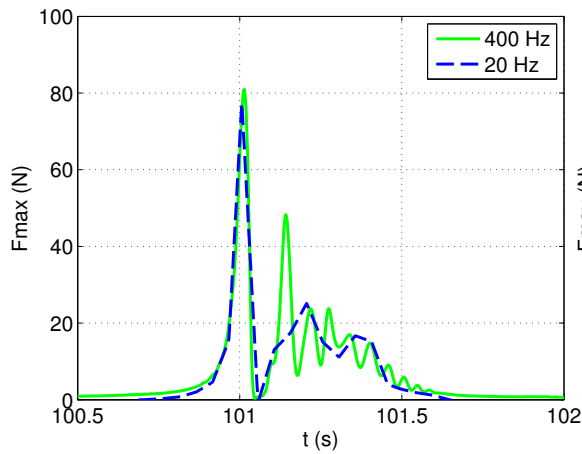


Figure C.1. Example of good fit by logging at 20 Hz.

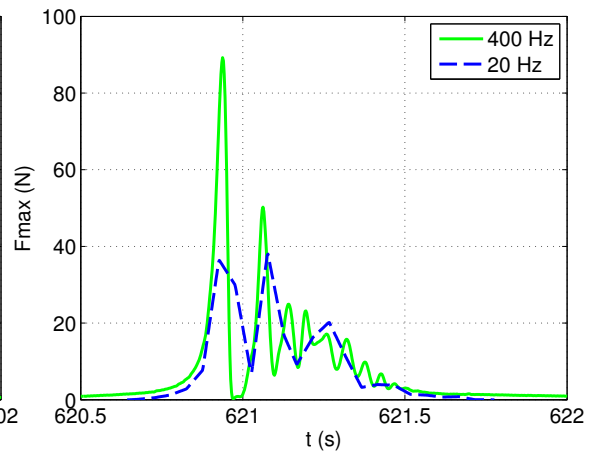


Figure C.2. Example of bad fitting by logging at 20 Hz.

Both figures show that the gauge logging at 400 Hz gives a better representation of the oscillatory loading of the chain, when excited with an impact load. When logging the peak load at an impact, it can be seen that in some cases the 20 Hz is sufficient. On the figure to the left, the logged value is close to the peak, while on the figure to the right, only one third of the peak load is logged. The same thing can be seen on the figure showing the entire time series. This gives a somewhat random representation of the loads, as the data logged at 20 Hz might and might not show the correct load.

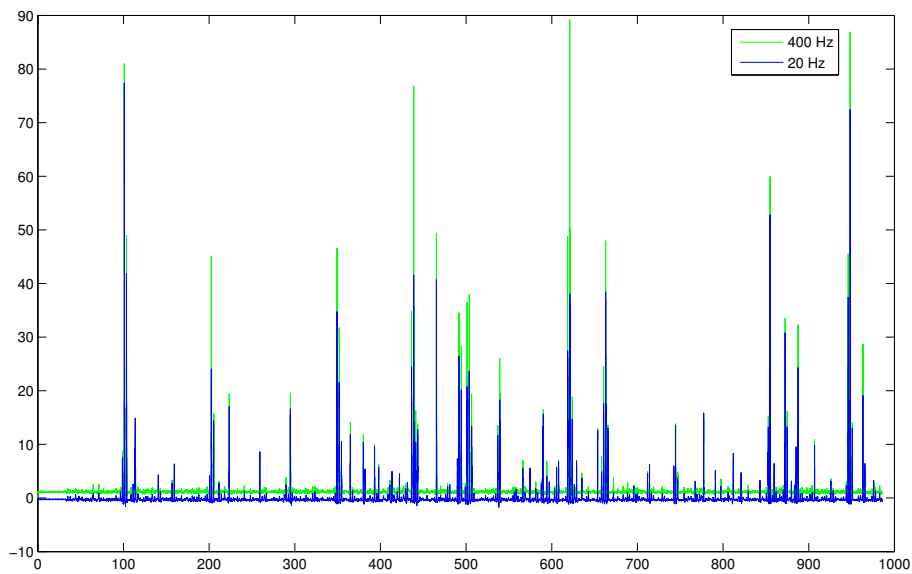


Figure C.3. Comparison of logged data for the entire time series.

D Analysis of movements

Results from the remaining tests:

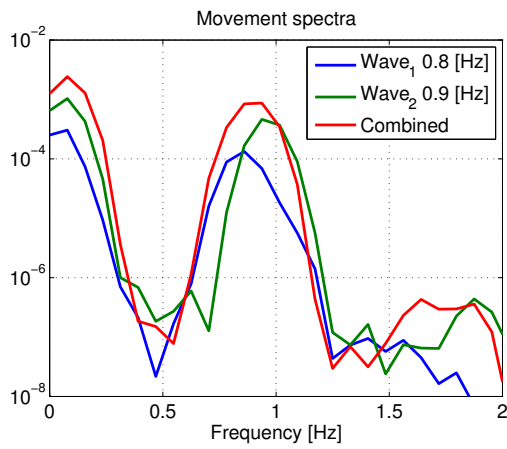


Figure D.1. Test 1,2 and 3 movement spectrum.

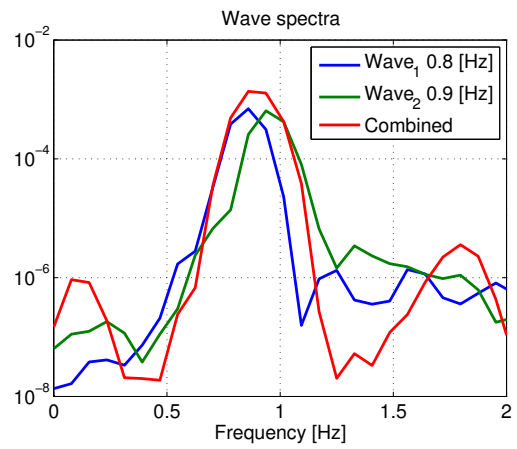


Figure D.2. Test 1,2 and 3 wave spectrum.

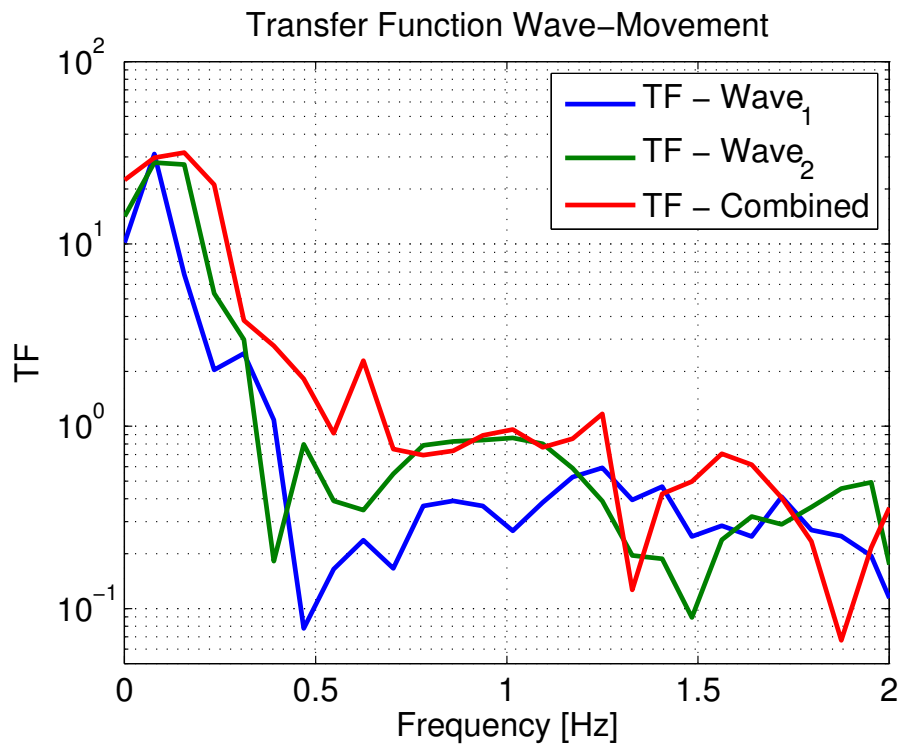


Figure D.3. Transfer function for test 1,2 and 3.

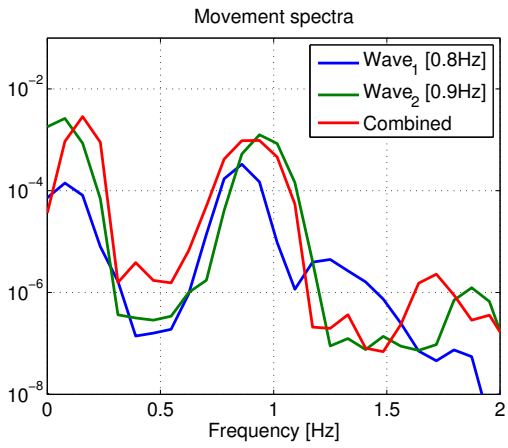


Figure D.4. Test 4,5 and 6 movement spectrum.

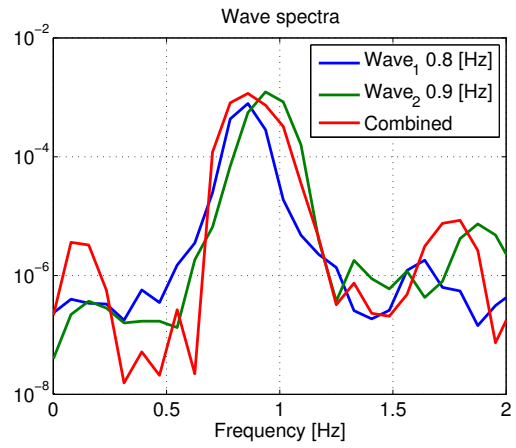


Figure D.5. Test 4,5 and 6 wave spectrum.

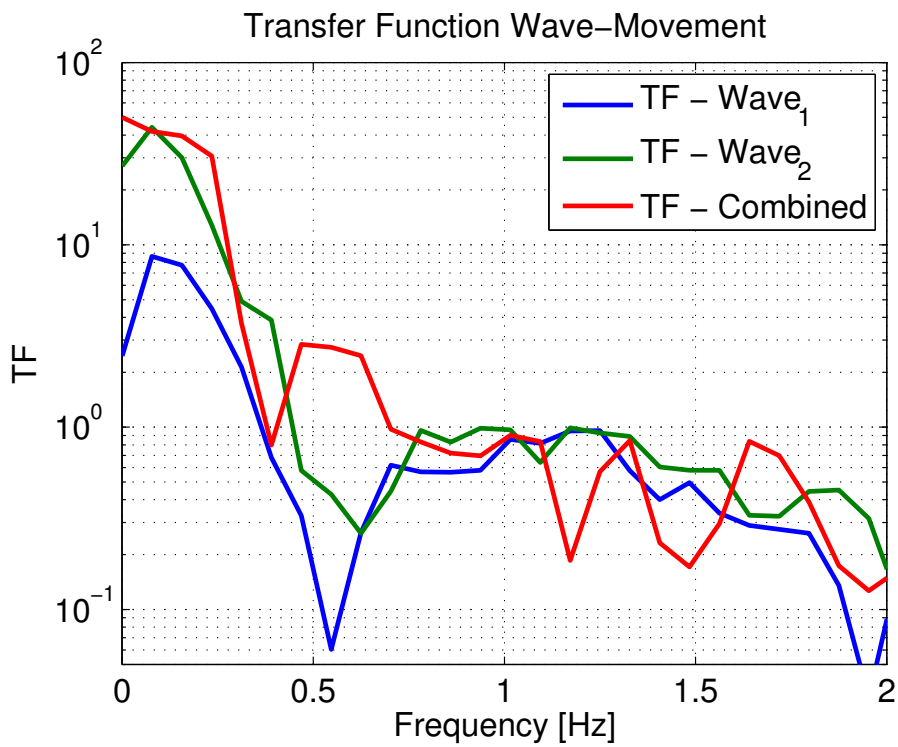


Figure D.6. Transfer function for test 4,5 and 6.

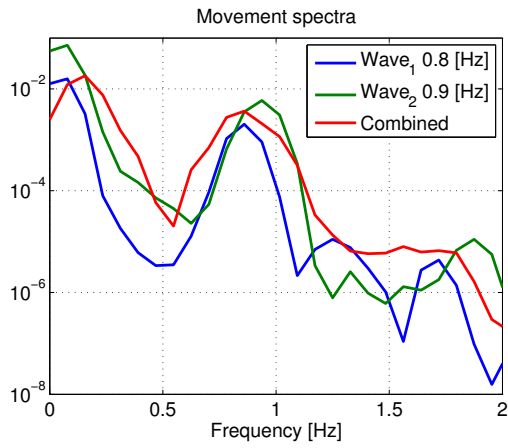


Figure D.7. Test 10,11 and 12 movement spectrum.

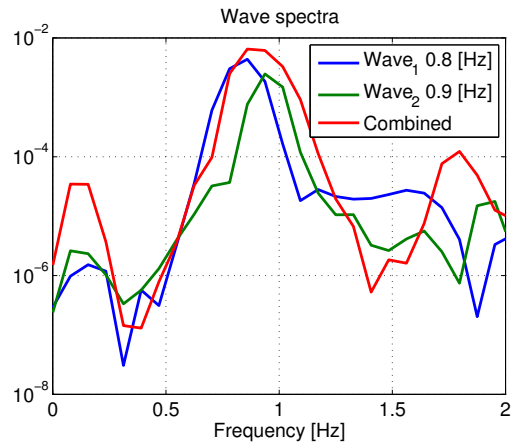


Figure D.8. Test 10,11 and 12 wave spectrum.

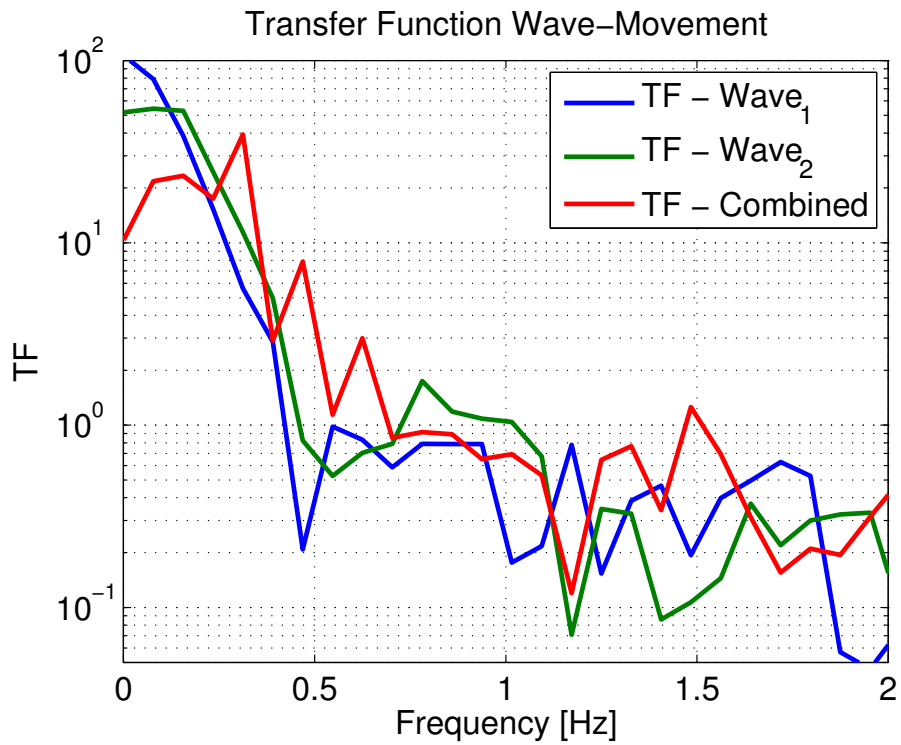


Figure D.9. Transfer function for test 10,11 and 12.